TECHNICAL SUMMARY REPORT

STUDY OF PROPERTIES OF HIGH-FIELD SUPERCONDUCTORS

AC Field Induced Flux Jumps

26 April 1966

Contract NAS 8-11272

Prepared by
APPLIED RESEARCH
DEFENSE ELECTRONIC PRODUCTS
RADIO CORPORATION OF AMERICA
CAMDEN, NEW JERSEY 08102

FOR

GEORGE C. MARSHALL SPACE FLIGHT CENTER
NATIONAL AERONAUTICS AND SPACE ADMINISTRATION
HUNTSVILLE, ALABAMA 35812

Technical Summary Report

Study of Properties of High Field Superconductors

AC Field Induced Flux Jumps

by D. A. Gandolfo
C. M. Harper

26 April 1966

Contract NAS 8-11272

Prepared by

Applied Research
Defense Electronic Products
Radio Corporation of America
Camden, New Jersey 08102

For

George C. Marshall Space Flight Center
National Aeronautics and Space Administration
Huntsville, Albama 35812

FOREWORD

This report was prepared by the Radio Corporation of America, Applied Research Department, Camden, N. J. under NASA Contract No. NAS-8-11272. Mr. E. W. Urban was the NASA Project Engineer.

This is a Technical Summary Report which describes progress during the period 21 June, 1965 through 26 April, 1966. The research work and report writing were done by D. A. Gandolfo and C. M. Harper of Applied Research, who were the Principal Investigators. G. D. Cody and R. Hecht of RCA's David Sarnoff Research Center, Princeton, N. J. served as consulants.

ABSTRACT 30752

Magnetization experiments in superimposed dc and audio frequency ac magnetic fields have been performed on tubular samples of cold worked Nb 50% Ti. The samples exhibited a dc field dependent critical-current density in agreement with Kim's equation. When an ac field whose amplitude exceeded a certain threshold was superimposed on the dc field, regular flux jumps ensued. The threshold was inversely proportional to the frequency, with the dependence being stronger at frequencies below 200 c/s. At low frequencies the duration of a flux jump was estimated as 2×10^{-4} sec. The flux jumps were identical in amplitude at a given frequency and strikingly similar from 6.3 to 208 c/s, the most common amplitude being in the range from 400 to 500 G. Temperature measurements made with a carbon resistor in the sample interior showed that threshold fields caused the bulk sample temperature to rise by not more than 0.1°K. This small increase is in qualitative agreement with computations of the steady-state temperature rise caused by hysteresis and eddy current losses, also found to be quite small.

TABLE OF CONTENTS

LIST OF ILLUSTRATIONS

LIST OF ILLUSTRATIONS (Continued)

Section I

INTRODUCTION

A. REVIEW OF PAST WORK

Work done in the past on this contract was concentrated on the study of the critical-current density and flux jumping in hard superconducting tubes and solenoids. These quantities were measured as functions of applied magnetic fields from 0 to 30kG and temperatures from 4.2°K to T_c. Hollow cylinders of Nb_3Sn, NbZr, and NbTi, and solenoids of NbZr wire and Nb_3Sn ribbon were investigated.[1]

At any fixed temperature below T_c, the critical-current density, J_c, in the wall of one of the hollow cylinders was found to be described by Kim's[2] equation, as long as critical-state data points could be obtained from magnetization curves. In Nb_3Sn samples at temperatures around 4.2°K, where J_c is large and flux jumps are numerous, a different approach was used to derive J_c. The values of magnetization at a flux jump were plotted against the applied field, H, and a "practical J_c" was derived. When these values of J_c were plotted against temperature, it was discovered that a maximum occurred near 8°K. This suggests that different mechanisms may trigger flux jumps at different temperatures. At T=14°K, flux jumps give way to pure critical-state performance.

The behavior of solenoids of Nb_3Sn ribbon and NbZr wire varied markedly. In the NbZr solenoids, flux jumps never occurred when flux was moving freely across the windings, i.e., when the sample was in the critical state. On the other hand, in the solenoids made of 0.090-inch wide Nb_3Sn ribbon, flux jumps occurred only after the sample had entered the critical state. These facts may indicate that different mechanisms trigger flux jumps in each type of solenoid.

In both types of solenoids the spacing (in the H' vs H plane) between flux jumps decreased if either magnetic field or temperature was increased. At higher temperatures the flux jumps were incomplete and were reduced to small excursions away from the critical state at higher values of magnetic field. Flux jumps were eliminated completely in the solenoid made of 0.090-inch wide Nb_3Sn ribbon at very high temperatures (12° to 16°K). In contrast, NbZr solenoids exhibited some flux jumps even at temperatures near T_c.

Flux jumps were sensitive to the magnetic field sweep rate in the Nb_3Sn solenoids and could even be eliminated at low values of temperature and field by employing quasi-static field sweep rates ($\approx$ 1 gauss/sec). The flux jumps in NbZr solenoids, on the other hand, showed little dependence on the field sweep rate and persisted for all rates used (1 to 100 gauss/sec).

B. SUMMARY OF PRESENT REPORT

Recently our interest has been focussed on the manner in which an alternating field penetrates a hard superconductor in which the mixed state has been established by the application of a dc field. Since the most interesting properties of hard superconductors are associated with the motion of flux lines (and the pinning of these lines by structural defects), it was felt that much could be learned from the study of a situation in which the lines are constantly excited, as by an alternating field. To this end, we have performed magnetization experiments on tubular specimens of NbTi using superimposed ac and dc fields. Section II of this report describes apparatus used in these experiments, especially the tickler coil which is the source of the ac field. Section II also discusses the calibration of the Hall probe used to measure the ac and dc magnetic fields and a technique by means of which the temperature of the specimen was measured during application of the ac field. In Section III the experimental results are described. In particular, we describe: (1) the dc critical-state characterization of the samples, (2) some

early results in superimposed fields obtained by means of an X-Y recorder, (3) results obtained by means of an oscilloscope which displayed the magnitude and waveforms of the ac field generated by the tickler coil and detected by the Hall probe, and (4) data bearing on the sample temperature during ac field application. Section IV discusses the interpretation of these results. The mode of penetration is identified as a flux jump and the dependence of the threshold for the onset of flux jumping on ac frequency and dc field strength is noted. A practical critical-current density for the ac field is computed. AC power losses in the specimen are considered in an attempt to identify the mechanism by which the flux jumps are triggered. The findings of this investigation as well as recommendations for further effort are contained in Section V.

Section II

EXPERIMENTAL APPARATUS

A. TICKLER COIL CHARACTERISTICS

A block diagram of the test setup for the study of ac field penetration into hard superconductors is shown in Figure II-1. In addition, the setup used to detect a temperature rise in the specimen (caused by the application of the ac field) is shown in inset A of Figure II-1.

The samples of niobium titanium used in this study were taken from a single ingot and machined into hollow cylinders 0. 51 cm in diameter and 3. 18 cm long. The wall thicknesses of these cylinders varied from 3.81×10^{-2} cm for sample 5a to 6.1×10^{-2} cm for samples 5 and 6. It is estimated that the finished samples were 75 per cent cold worked. The samples had the following chemical composition:[3]

Material	Amount/Sample
Niobium	50. 2 percent by weight
Titanium	49. 8 percent by weight
Oxygen	1343 ppm by weight

The tickler coil used to generate the ac magnetic field was composed of approximately 2000 turns of No. 38 copper wire in 10 layers over the length of a 3. 15 cm long coil. The dimensions of the tickler coil were chosen to be compatible with those of the heater cavity, described in the previous technical summary report[1]. At room temperature the resistance of the coil measured 100 ohms and the inductance 7 mH. At 4. 2° K the resistance measured 1 ohm while the inductance, with no sample in position, remained at 7 mH. However, with the superconductive

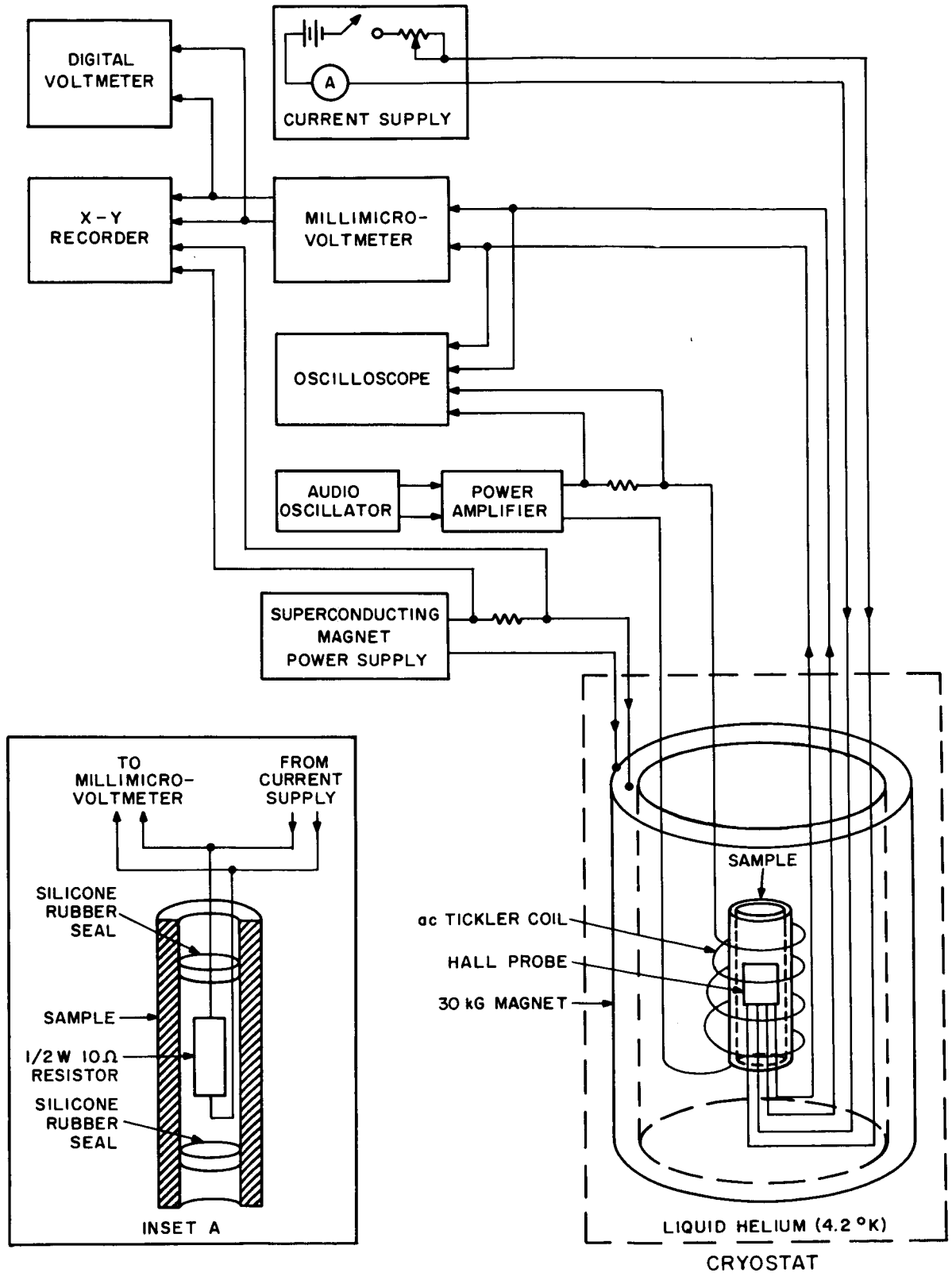

Figure II-1. Equipment Arranged in Configuration Used for Magnetization Experiments in Superimposed AC and DC Fields. Inset Shows Arrangement Used to Measure Specimen Temperature.

sample in position, much of the interior volume of the coil was excluded by the flux shielding properties of the specimen and the inductance was reduced to 3.6 mH.

Using the usual expression for a long solenoid, a field of 960 gauss per ampere was computed for the tickler coil. One ampere rms of current will dissipate one watt of power in the tickler coil at 4.2° K. This can be absorbed by the He bath with no temperature increase in the coil.

Four narrow strips of 0.025-cm thick mylar were cemented along the length of the outer surface of each NbTi sample. The samples were then inserted into the interior of the tickler coil. The 0.025-cm space allowed helium to flow between the specimen and the coil to insure that no heating of the sample would occur as a result of power dissipated in the tickler coil.

A Hall probe was inserted into the interior of the NbTi tube to measure internal magnetic field intensity, and the coil-sample-probe assembly was lowered into the center of a 30 kG superconducting magnet. The entire apparatus was immersed in liquid helium.

In a typical experiment, a dc magnetic field was applied while the magnetization was displayed on a X-Y recorder. Thus, with the mixed state established the sample was ready for an ac field to be applied.

An audio signal was fed from the audio oscillator to a power amplifier which drives the low impedance tickler coil. The current through the tickler coil was measured by means of a 0.01-ohm resistance in series with the coil. With proper calibration the voltage developed across this resistance may be directly related to the ac magnetic field generated by the tickler coil.

Displaying the voltages from the output of the Hall probe and the 0.01-ohm resistor on an oscilloscope permitted one to compare the amplitude and wave

shape of the applied ac magnetic field to those of the ac magnetic field which penetrated to the interior of the NbTi sample.

Direct current magnetization curves for these superconducting samples were plotted on the X-Y recorder with the dc magnet current driving the X coordinate (abscissa) and the dc Hall probe voltage driving the Y coordinate (ordinate).

B. TEMPERATURE MEASUREMENTS

The temperature of the sample during the application of the ac field was measured by means of a 1/2 watt carbon resistor with a nominal resistance of 10 Ω at room temperature. The resistor was stripped of its insulating jacket (to improve its thermal contact with its environment) and covered with a thin coat of varnish for electrical insulation. Resistance vs. temperature was computed from the expression[4]

$$\frac{(\log_{10} R - b)^2}{\log_{10} R} = \frac{a}{T}$$

Measurements of resistance at 77° and 4.2° K permitted us to evaluate the constants a and b. (Actually the resistance change between 77° and 4.2° is too large to permit a really accurate evaluation of these constants, but this procedure is good enough to justify the semi-quantitative conclusions we make regarding sample temperature.) The resistor was placed inside the sample and the ends of the tube were sealed with silicone rubber after the volume surrounding the resistor was filled with apiezon grease. This provided good thermal contact between the resistor and the interior surface of the sample and prevented the resistor from making contact with the liquid helium. Resistor leads were brought out through one of the seals and connected to a low current supply as shown in inset A of Figure II-1. The sensitivity of the resistor at 4.2° K was approximately 40 Ω /degree. The resistor measured the same in a dc field of 10 kG as it did in 0 field.

C. HALL PROBE CALIBRATION

It was found that the response of the Hall probe could be made more linear for use with dc magnetic fields by increasing the current from 6 to 25 mA. Above 25 mA, the Hall probe voltage saturated in a 25 kG field, rendering it unuseable.

Figure II-2 was plotted with a Hall current of 25 mA. The probe sensitivity $\frac{dH}{dV_H}$ equals 613 gauss/mV at H = 0 and 500 gauss/mV at H = 10 kG. Nevertheless, the linearity is good above 7 kG except for a point at 24 kG. Data taken with a Hall current of 6 mA resulted in a curve which had deviations from linearity several times greater than those shown in Figure II-2. This increase in operating current proves no disadvantage in heat dissipation, since in a 30 kG field, only 1 mW of power is dissipated in the Hall probe.

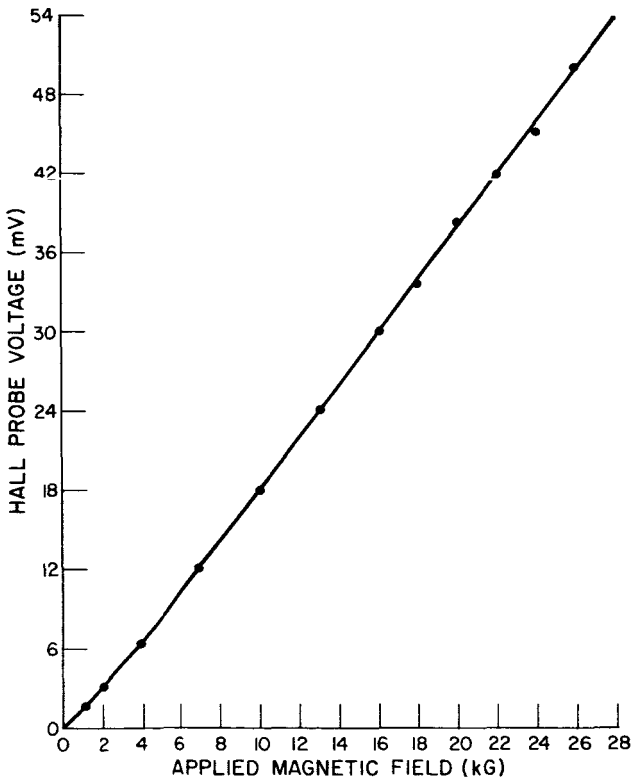

Figure II-2. Hall Probe Calibration Curve Showing Hall Voltage as a Function of the DC Magnetic Field.

The Hall probe played a significant roll in this experiment by revealing the amplitude and wave form of the ac magnetic field which reached the interior of the superconducting sample. For this reason the ac calibration of the Hall probe was determined in the following manner.

The Hall probe was inserted into the tickler coil but no sample was in position. A Hall probe current of 25 mA was used and the Hall voltage was displayed on an oscilloscope. The amplitude of the signal on the tickler coil was held constant while the frequency was changed. Under these conditions it was observed that the signal appearing on the Hall probe was sinusoidal and constant from 5 to 500 c/s and within 7% of constant from 500 to 2000 c/s. Using the dc Hall probe sensitivity we found that the tickler coil produced a field of 1140 gauss/amp. This value was used in analyzing subsequent data.

Section III

DESCRIPTION OF EXPERIMENTAL DATA

A. CRITICAL-STATE DATA

The critical-state characteristics of the samples have been derived from magnetization experiments using the apparatus depicted in Figure II-1 and described in detail in a previous report [1]. In these experiments the field in the interior of the specimen, H', is measured as a function of the applied field, H, which is varied slowly over the range 0-to-25,000 gauss. Graphs of H' vs. H for the three specimens are shown in Figures III-1 (sample No. 5), III-2 (sample No. 6), and III-3 (sample No. 5a).* The quantity $(H - H')$, used in computing the critical-current density, is obtained from these graphs.

From Maxwell's equation, which in the presence of steady fields is,

$$\nabla \times H = \frac{J}{0.4\pi}$$

where

H = magnetic field intensity in gauss

J = current density in amps/cm^2

it can be found that the critical-current density for a specimen of wall thickness, w, is given by

$$J_c = \frac{(H - H')}{0.4\pi w}$$

Typical values of J_c for several values of H are given in Table III-1. The critical-state data in the range of interest are reasonably well described by Kim's semi-empirical expression:

*The waviness of these curves was caused by the nonlinear response of the Hall probe; a probe current of 6 mA was being used when these curves were obtained.

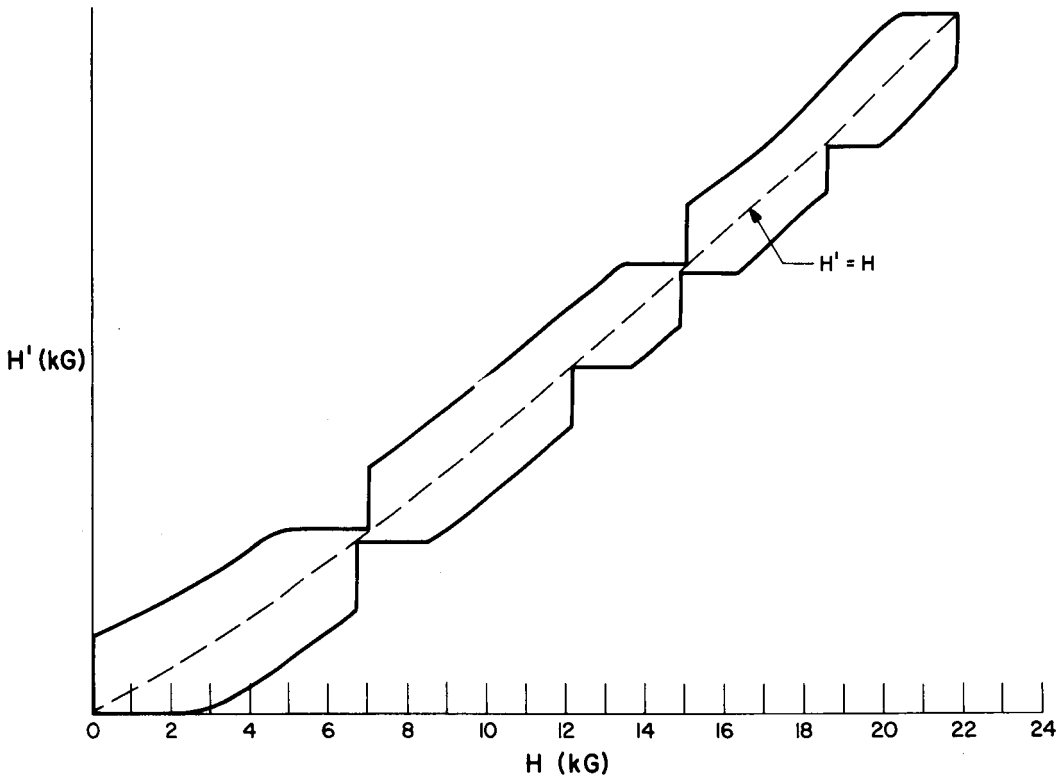

Figure III-1. Critical State Curve for Sample 5 in a Slowly Changing Magnetic Field.

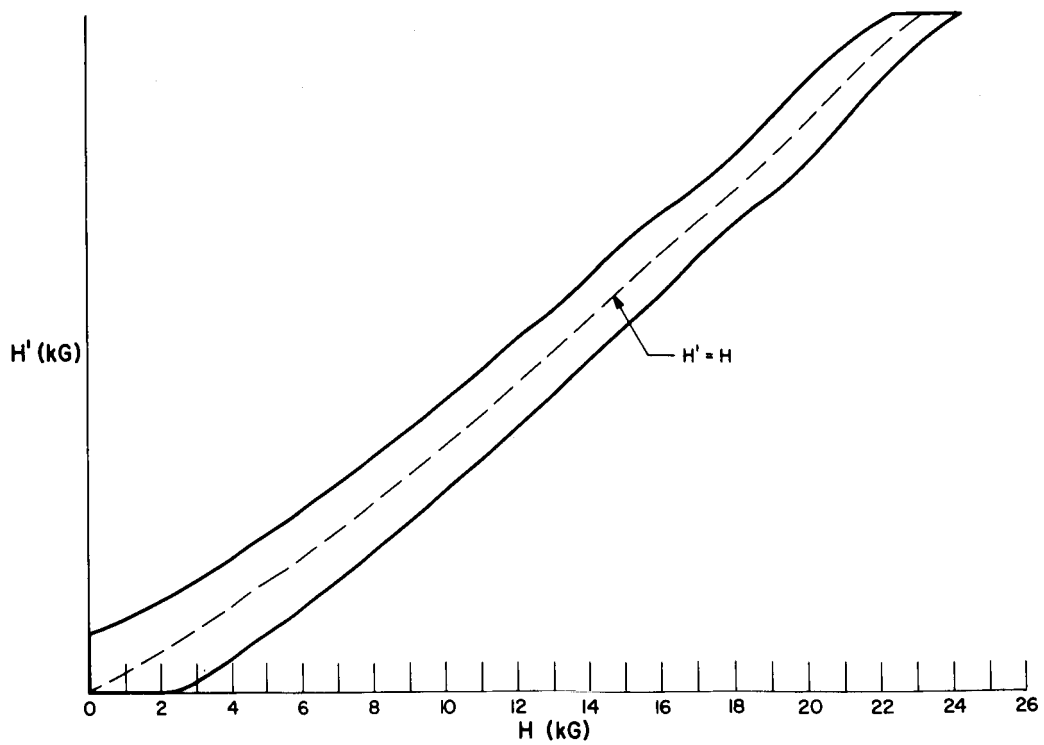

Figure III-2. Critical State Curve for Sample 6 in a Slowly Changing Magnetic Field.

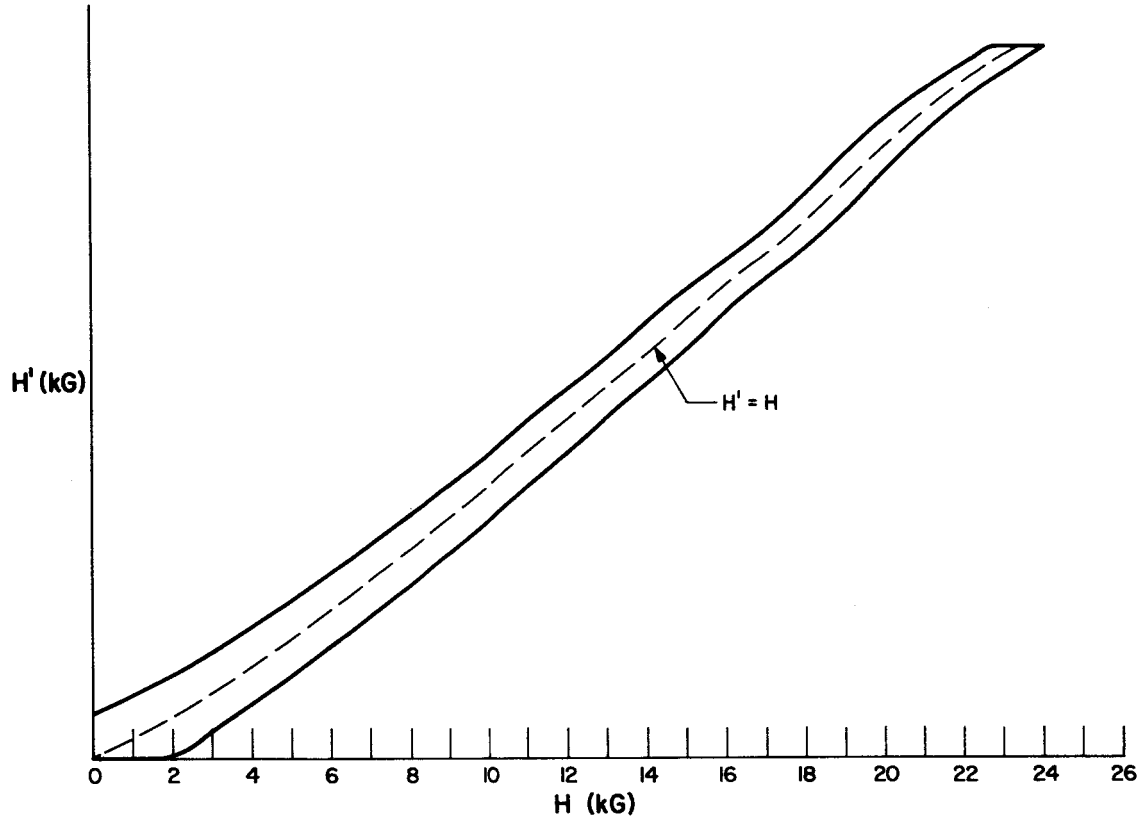

Figure III-3. Critical State Curve for Sample 5a in a Slowly Changing Magnetic Field.

$$J_c = \frac{\alpha_c}{H^* + B_o}$$

where

α_c = a constant related to the strength of pinning centers in the specimen

B_o = a constant related to the lower critical field H_{c1}

H^* = the average field in the specimen wall

A graph of $1/J_c$ vs. H^* yields a straight line which has a slope equal to $1/\alpha_c$ and a Y-axis intercept equal to B_o/α_c. These quantities have been computed for the specimens used in this experiment, and their values are listed in Table III-1.

TABLE III-1. SUMMARY OF CRITICAL-STATE DATA

Sample No.	w (cm)	J_c (A/cm^2)			$\left(\frac{\alpha_c}{\frac{kG-A}{cm^2}}\right)$	B_o (kG)
		5 kG	10 kG	20 kG		
5	6.1×10^{-2}	3.8×10^{4}	2.7×10^{4}	2.1×10^{4}	0.63×10^{6}	13.2
5a	3.8×10^{-2}	2.9×10^{4}	2.1×10^{4}	1.5×10^{4}	0.46×10^{6}	11.0
6	6.1×10^{-2}	2.9×10^{4}	2.2×10^{4}	1.6×10^{4}	0.43×10^{6}	11.2

Figure III-4 shows how the critical-current density is expected to vary as a function of temperature. It may be noted that the form of the temperature dependence bears a reasonably close similarity to Anderson's[7] predicted variation of α_c with T.

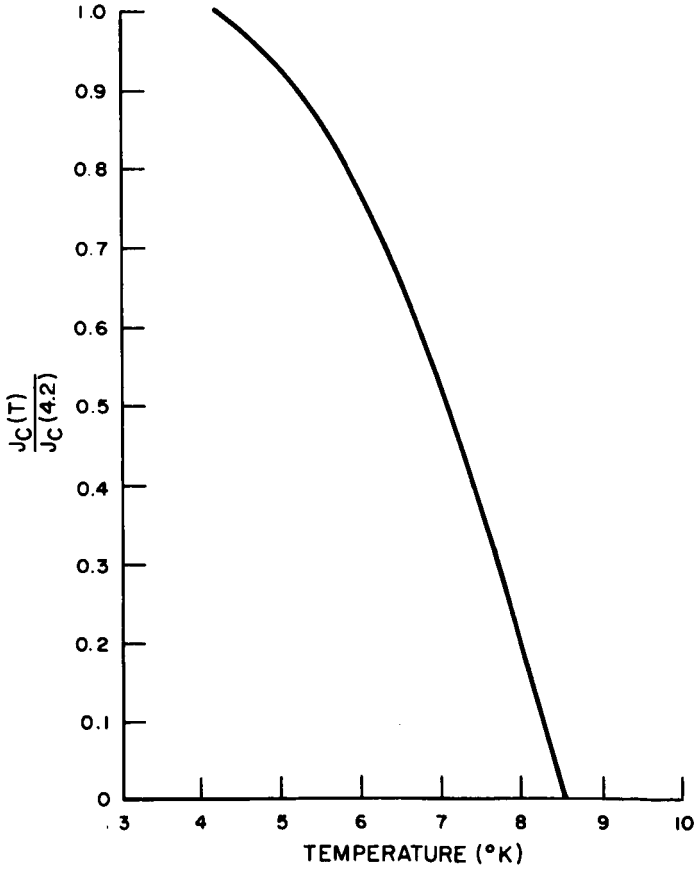

Figure III-4. Normalized Temperature Dependence of the Critical Current Density of a Typical NbTi Specimen in a Small (i.e. Several Kilogauss) Magnetic Field. (Based on data from reference 1, page 18.)

The dc critical-state data all serve to demonstrate that the specimens are well-characterized, well-behaved representatives of the class of hard superconductors.

B. EARLY OBSERVATIONS OF AC FIELD PENETRATION (WITH X-Y RECORDER DISPLAY)

In the early experiments the output of the Hall probe was fed to an X-Y recorder which permitted tracing the critical state (as the dc field was slowly increased or decreased). The typical experimental procedure was as follows: 1) The critical state was established by the application of a dc field of from 2000-to-25,000 gauss; 2) The ac field was applied and its amplitude, at the moment when an ac component reached the Hall probe, was recorded; the presence of the ac component at the probe was indicated by a rapid fluctuation of the, heretofore quiescent, pin on the X-Y recorder.

Data showing h_1, the amplitude of h when ac first appears at the Hall probe, as a function of the frequency and as a function of the dc field, were obtained. These data were consistent with those obtained later with the Hall probe output displayed on an oscilloscope, although the numbers are believed to be less accurate because of the inherently lower sensitivity of the X-Y recorder. These data are summarized in Figures III-5, III-6 and III-7. The figures refer respectively to sample No. 5, sample No. 5a, and sample No. 6. h_1 as seen in these figures shows a definite, although weak, dependence on frequency and dc field strength. The dc field dependence is qualitatively similar to that of the critical current-density, J_c, being stronger at low fields (less than 5,000 gauss). It is of interest to compare the data from sample 5a with those from the thicker-walled samples 5 and 6. On the basis of the linear, field-dependent penetration depth, which characterizes the mixed state of a hard superconductor, it is expected that a greater field will be required to penetrate a thicker specimen. This expectation is clearly not borne out by Figures III-5, III-6, and III-7. The solution to this problem is provided by the oscilloscope data which show that the penetration of the ac field into the interior of the specimen occurs by means of flux jumps. Once this is recognized, a simple, linear dependence of h_1 on the sample wall thickness is no longer expected.

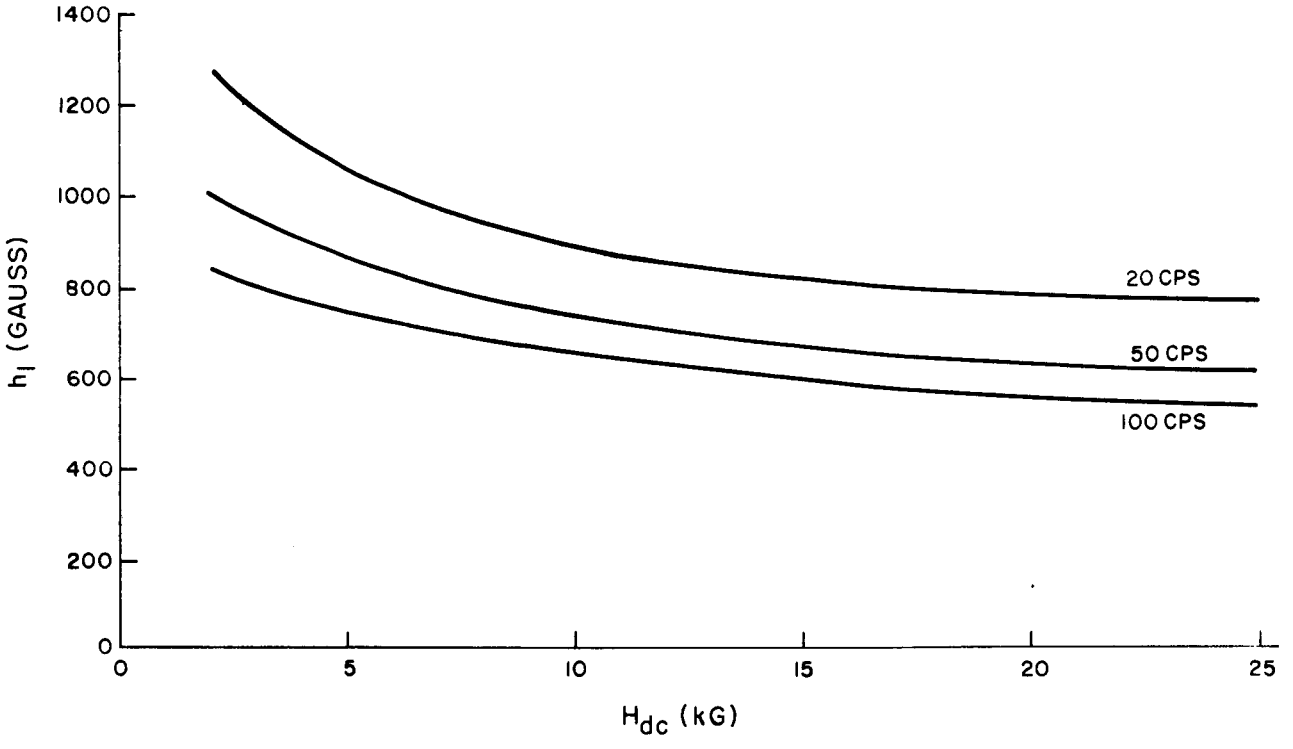

Figure III-5. h_1, the Amplitude of the Applied Field When an ac signal Reaches the Hall Probe, as a Function of the dc Field, With the Frequency as a Parameter (Data for Sample 5).

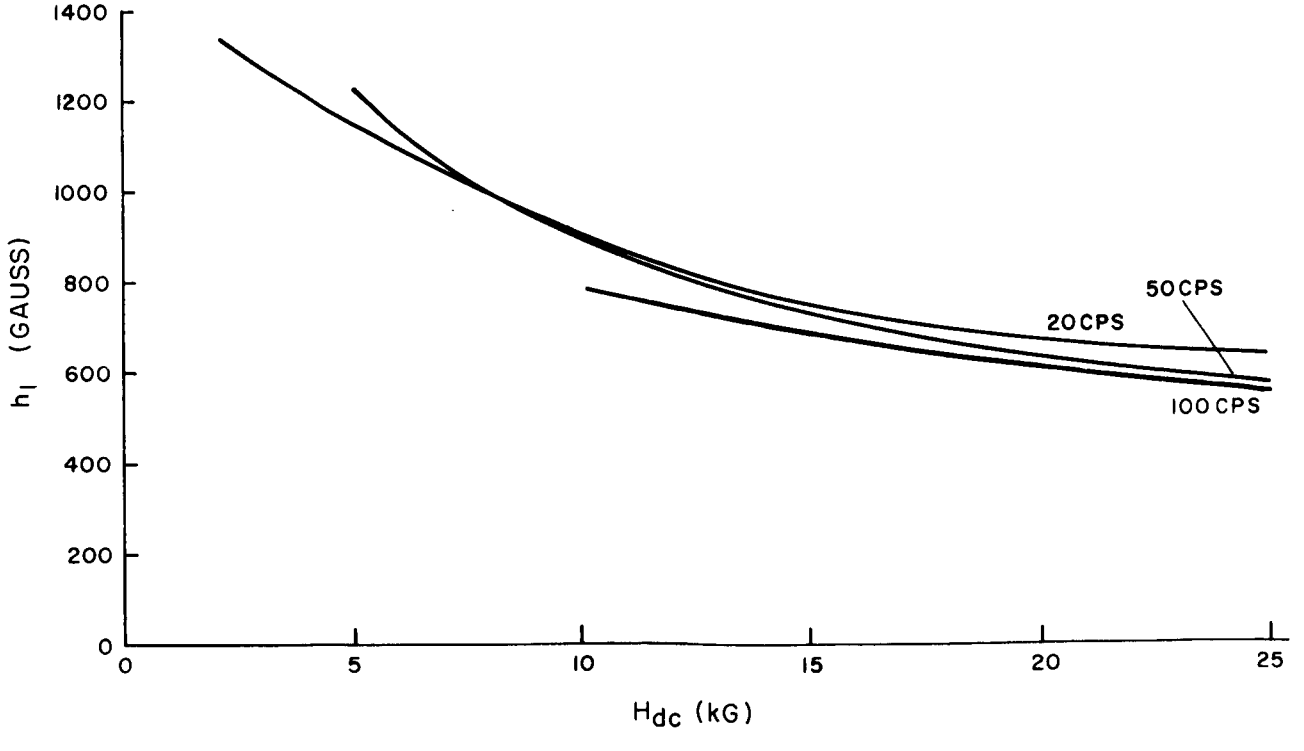

Figure III-6. h_1 Versus H_{dc} With Frequency as a Parameter (Data for Sample 5a).

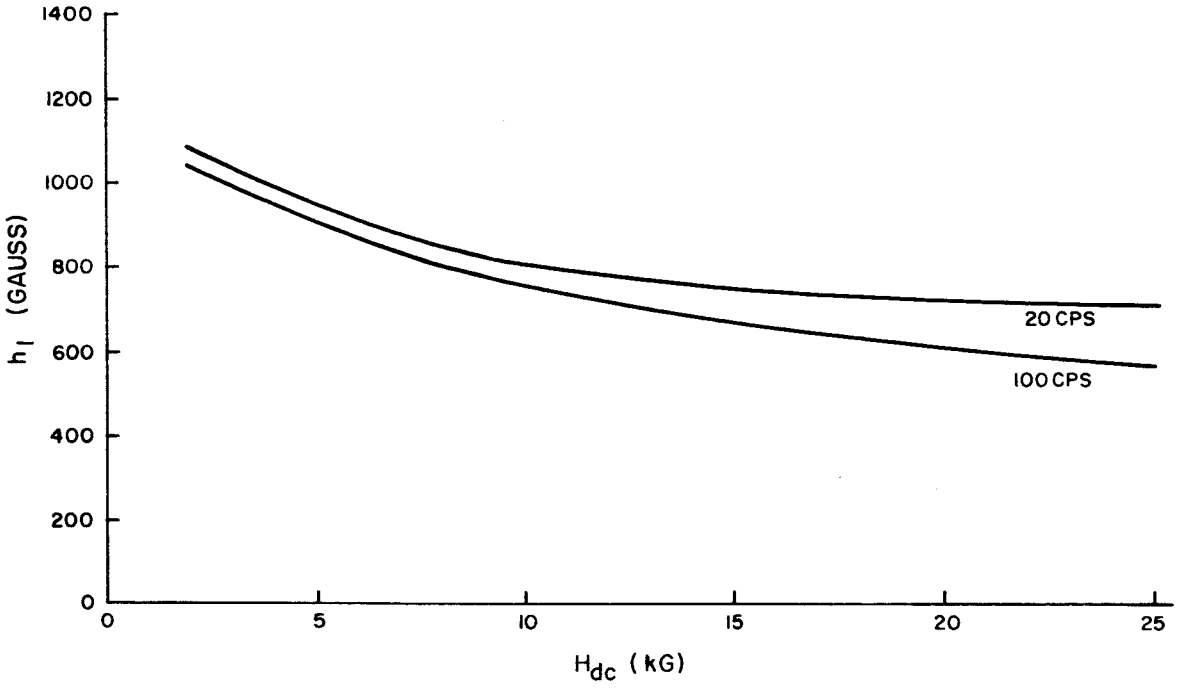

Figure III-7. h_1 Versus H_{dc} With Frequency as a Parameter (Data for Sample 6).

C. OBSERVATIONS OF AC FIELD PENETRATION (WITH OSCILLOSCOPE DISPLAY)

Early results demonstrated that in order to interpret the ac field penetration data we would have to know the waveform of the signal which actually appeared inside the specimen. Therefore an attempt was made to display on an oscilloscope both the signal generated by the tickler coil and the signal that penetrated the specimen and was detected by the Hall probe. The results proved most interesting. Two distinct modes of penetration were observed. These are referred to as the square wave mode and the sine wave mode. The square wave mode was observed at frequencies up to several hundred c/s while the sine wave mode was observed at higher frequencies.

A typical sequence of events in the square wave mode is shown in the oscilloscope photographs in Figure III-8 (a) (b) (c) (d). The applied signal, h, is on the lower trace and the signal reaching the Hall probe, h', is on the upper trace in these and in all other photos unless otherwise noted. The mixed state was established in the specimen by the application of a static field of, in this case, 10 kG. The ac field was then applied by means of the tickler coil. The amplitude of h in

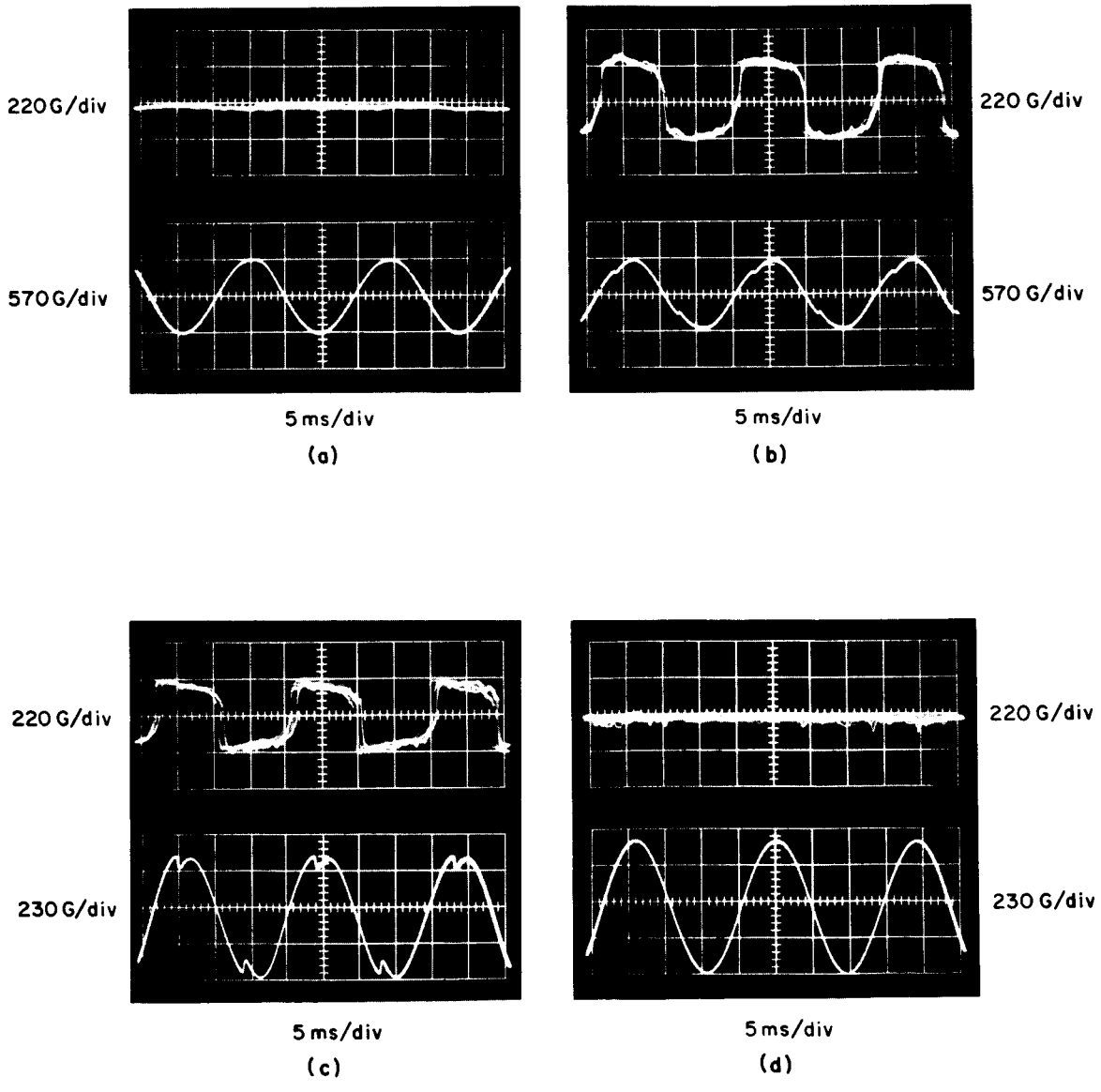

Figure III-8. Penetration of an ac Field to the Interior of a Tubular Sample - - a Typical Experimental Sequence

Figure III-8 (a) is just below the threshold required to cause an ac component to appear on the Hall probe and one notes on the Hall probe trace that $h' = 0$. The amplitude of h is about 1140 gauss (peak-to-peak). The scope sensitivity used for the Hall probe trace corresponds to 220 gauss/cm but we have made the same observation using a sensitivity of 25 gauss/cm; thus it can be confidently concluded that no ac component has reached the probe. A very slight increase in h was sufficient to cause an ac component to appear on the Hall probe and this is shown in Figure III-8 (b). It can be seen that the signal reaching the probe is a square wave. (Subsequent work shows that it is truly square and that the rounding-off of the sharp corners in this photograph is caused by the oscilloscope bandwidth used.) The rise time of these pulses is much shorter than any to be found in the applied signal. This indicates that flux was rushing into and out of the specimen in a discontinuous fashion, i.e., flux jumps were occurring. The plateau regions indicate that during a portion of the cycle the field in the interior of the specimen was not changing although the external field was changing; thus, there was still shielding and the sample was still superconductive except at the instant during which flux rushed in or out. The frequency of the square pulses was identical to that of the applied signal. The amplitudes of all the square pulses were identical. This is considered noteworthy since it indicates that the flux jump is occurring in the same manner each time and is thus quite reproducible in magntiude and temporal characteristics. Flux jumping is generally thought to be a random phenomenon and this may be so in the sense that each sample may require different conditions. It appears, however, that for a given sample the conditions required to cause a flux jump are a fundamental property of the sample. This has been observed even when the dc field is increased quasi-statically, for one notes flux jumps occurring repeatedly at the same point in the H' vs. H plots. Note of this was taken in the last technical summary report. [1] In the lower trace of Figure III-8 (b), one notes that the wave form of the applied signal underwent a slight but significant modification when a flux jump occurred. This modification consisted of small pips on both the increasing and decreasing portions of the wave form. The time between these pips corresponded precisely to the

duration of the plateaus of the square pulses appearing on the Hall probe trace. These pips were caused by the rapidly varying inductive load which the tickler coil presents when flux penetrates the specimen. Recall that the inductance of the coil is directly proportional to the cross-sectional area threaded by magnetic flux. Since magnetization currents shield the bore of the superconductive specimen, the flux generated by the tickler coil is excluded from a large fraction of the cross section (except during flux jumps). During the flux jump, a portion of the specimen returns to the normal state allowing flux to enter the formerly shielded region. When this new area becomes available to the coil, its inductance increases rapidly. Since the power amplifier supplies a fixed voltage to the tickler coil, the suddenly increased inductive reactance results in a decrease in current through the coil.

Once the threshold value of the applied signal has been exceeded and regular flux jumping has begun, we may reduce the amplitude below the original threshold value and note that flux jumps still occur in the same manner but with a slightly reduced amplitude. This phenomenon is exhibited in Figure III-8 (c). This picture can be compared with Figure III-8 (a) and it is seen that flux jumps are being sustained by a signal amplitude which is only 68 percent of the original threshold. It can also be noted that in the lower trace of this figure, the pip which marks the time when the flux jump occurs has moved closer to the peak of the ac signal as might be expected. A further reduction in applied signal amplitude causes flux jumps to cease completely as can be seen in Figure III-8 (d).

The square wave mode has been observed at 6.3, 22, 53, and 208 c/s in static fields of 5, 10, and 20 kG. The 10 kG data are shown in Figure III-9 (a, b, c, and d) for f = 6.3, 22, 53, and 208 c/s, respectively. Distortion of the applied signal and oscilloscope synchronization proved to be troublesome at the lowest frequencies (6 and 22 c/s); however, the data are still useful. It may be noted that all the photographs in this figure exhibit the characteristics discussed earlier, especially the square waves on the Hall probe trace and the pips on the applied signal trace which occur at the flux jump. The upper and lower traces in each photograph were taken

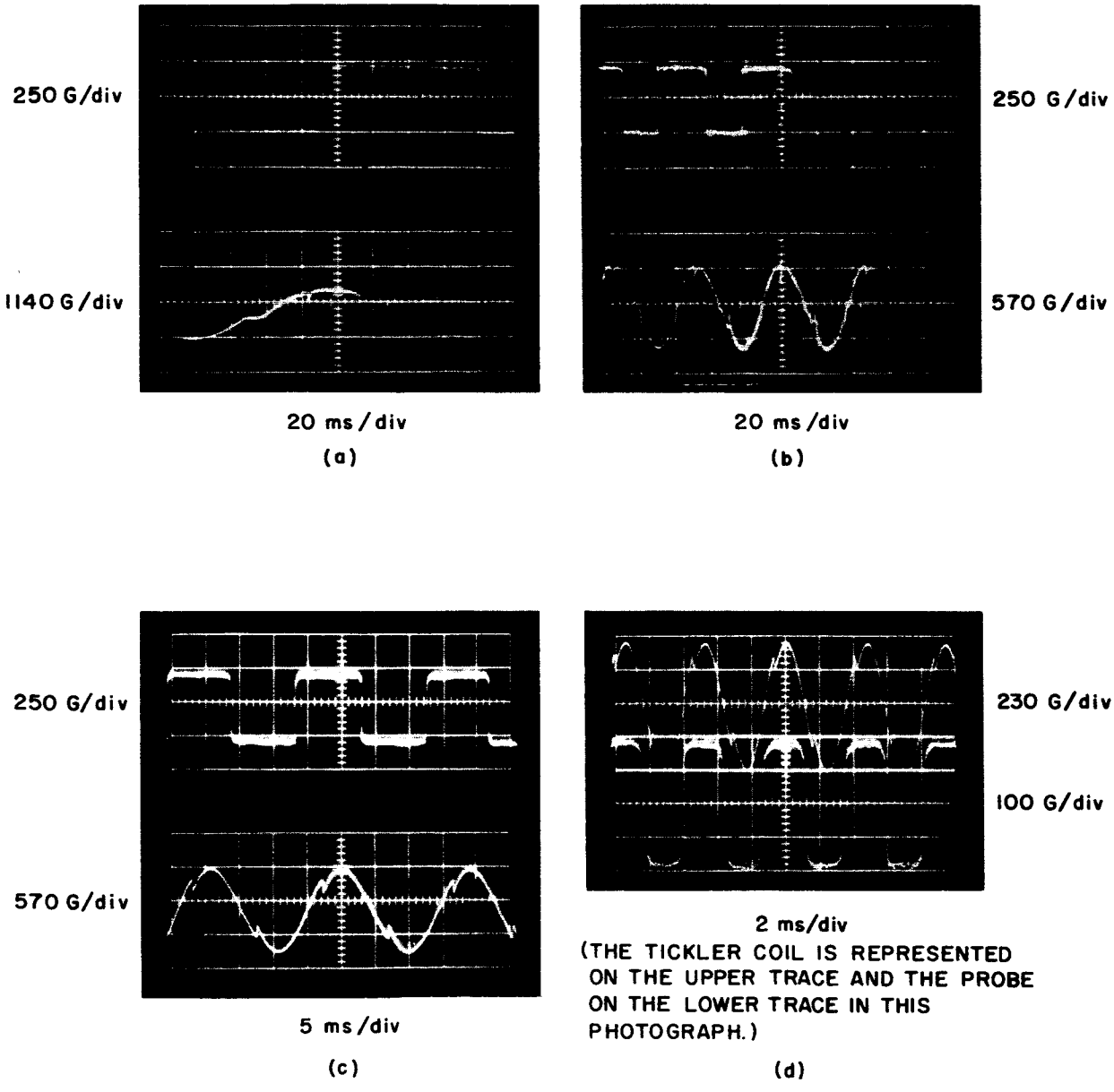

Figure III-9. Flux Jumps (Square Wave Mode) in Sample 5a Induced by the ac Field at f = 6.3 c/s (a), 22 c/s (b), 53 c/s (c) and 208 c/s (d)

sequentially not simultaneously. For this reason the pips on the applied signal traces do not line up with the sides of the square pulses; however, comparison of the times between pips with the duration of the square pulses convinces one that the two occur simultaneously. A noteworthy feature of these photos is that pips on the applied signal trace are not necessarily symmetrical about the peak of the signal as might be expected. This is most noticeable in the photo at 22 c/s where one pip appears near the positive peak while the other appears midway between the zero-crossing and the negative peak. Apparently the flux jumps from the shielding state and trapping state occurred under slightly different ac field conditions. Note that the duration of the plateau regions of the square pulses underwent a "long-short" alternation just as the time between pips in the applied signal was long or short.

In addition to the above, data have been obtained at 53 c/s in static fields of 5 and 20 kG. These data normalized to the 5 kG value are summarized in Table III-2; they show how the threshold ac field varies with the static field.

TABLE III-2. NORMALIZED h, AT THRESHOLD FOR FLUX JUMPS, FOR SOME VALUES OF H (SAMPLE 5a)

H (kG)	h/h(5 kG)
5	1.00
10	0.74
20	0.56

Flux penetration in the sine wave mode was similar to that in the square wave mode in that the ac field had to be increased to a certain threshold before an ac component appeared in the interior of the specimen. It differs in an important respect, however. When the threshold value was exceeded, a signal of form identical to that of the applied signal and of nearly identical amplitude appeared at the Hall probe. There was no shielding of a portion of the signal by the sample, as

occurred in the plateau region of the square waves. Except for a slight decrease of amplitude, the signal appears to have been unchanged by any interaction with a superconductive specimen. Examples of the behavior are shown in Figure III-10 (a, b, c, and d) for frequencies of 53, 500, 1040, and 2080 c/s, respectively. Although the sine wave mode is primarily a higher frequency phenomenon (i.e., f > several hundred c/s), it is possible to produce this effect at lower frequencies (as in Figure III-10 (a) at 53 c/s) by increasing the amplitude of h well beyond that required to cause flux jumps initially.

In this mode, as in that discussed earlier, it was possible to reduce the amplitude of the applied signal to a value smaller than the original threshold and still observe an ac component at the Hall probe. If h was made small enough, the form of the signal at the detector approached that of a square wave as shown in Figure III-11 (f = 1040 c/s). The flattened top of h' indicates that some shielding is occurring during the time when h is near its peak values, and therefore most slowly varying. No shielding occurs during the remaining portions of the cycle as indicated by the manner in which the detected signal follows the applied signal. A further decrease in h beyond this point causes the ac component to disappear from the detector discontinuously.

As mentioned earlier it was possible to cause h' to become sinusoidal at very low frequencies (less than several hundred c/s) by making h large. The transition from square wave to sine wave behavior with increasing field in the low frequency regime is also of interest. If h was increased, even after square waves appeared on the detector (refer to Figure III-9), a multitude of flux jumps, comparable in amplitude to the first one, were produced. Representative examples of this behavior are shown in Figure III-12 at 6.3, 22, and 53 c/s. In these photos each flux jump appearing on the h' trace is accompanied by a pip on the h trace and the time between pips is identical to the duration of the shielding behavior between flux jumps. The longest period of shielding occurs near the peak of h when the applied signal is most slowly varying. The approach of h' to a sinusoidal form is apparent in all photos.

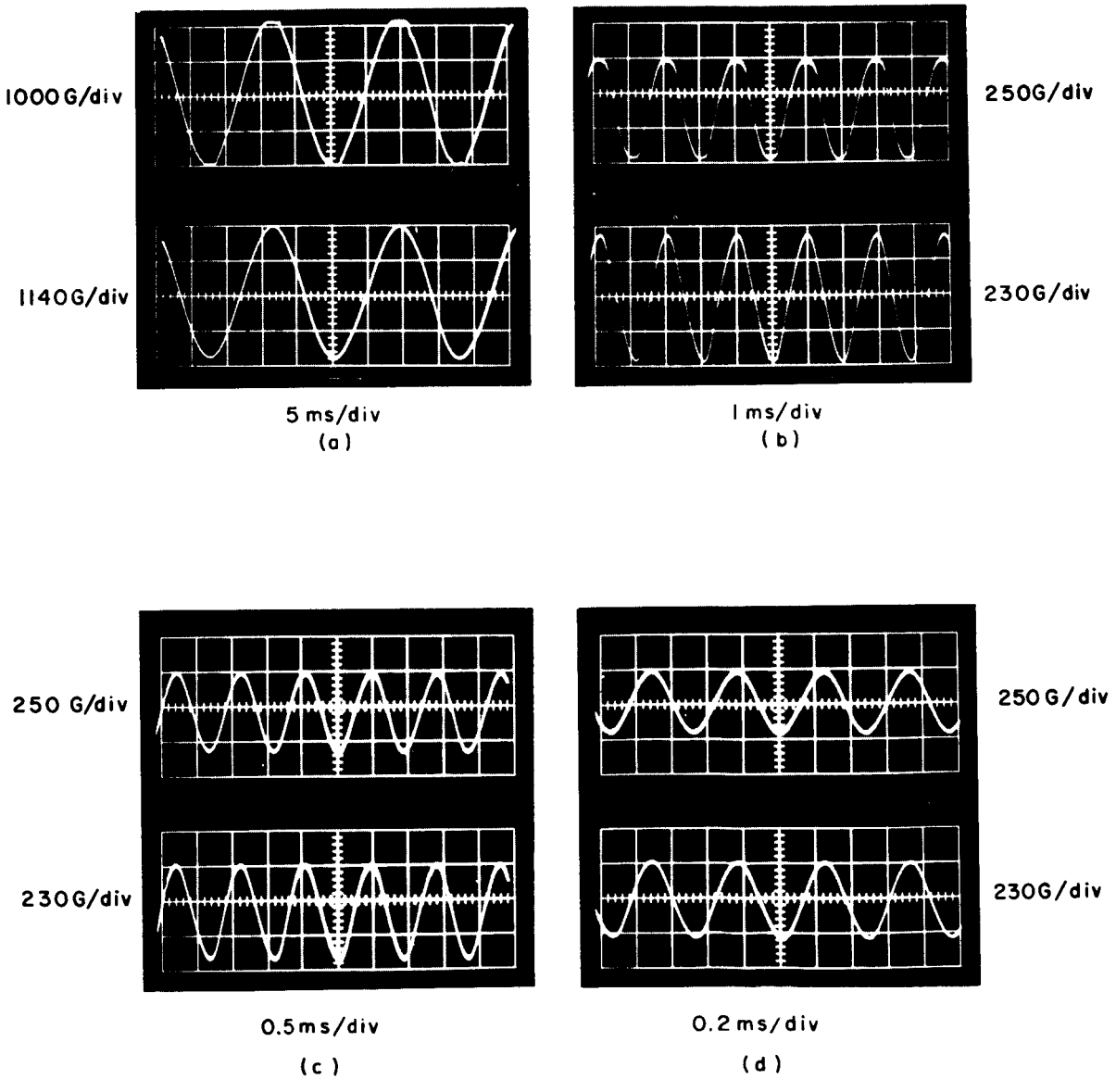

Figure III-10. AC Field Penetration (Sine Wave Mode) into Sample 5a at f = 53 c/s (a), 500 c/s (b), 1040 c/s (c) and 2080 c/s (d)

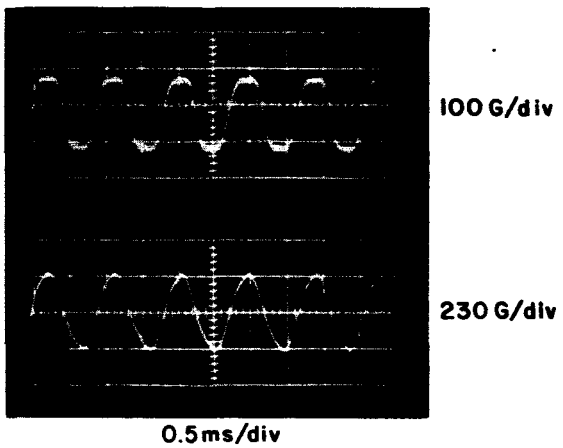

Figure III-11. ac Field Induced Flux Jumps at f = 1040 c/s after h Has Been Reduced below Original Threshold

A complete sequence from the first appearance of square waves on the detector through the appearance of the sinusoidal signals is seen in Figures III-9 (c), III-12 (d), and III-10 (a) for f = 53 c/s.

D. TEMPERATURE MEASUREMENTS DURING APPLICATION OF AN AC FIELD

A calibrated carbon resistor mounted in a sample (see Figure II-1) was used to monitor the temperature of the specimen during the application of the ac field. Since the properties of hard superconductors are strongly temperature sensi-sensitive even at temperatures well below T_c, the specimen temperature is of great interest. The tickler coil-sample-resistor assembly was immersed in liquid helium and a field of 10 kG was established by the dc solenoid. The tickler coil was then energized and the voltage across the carbon resistor, at a fixed

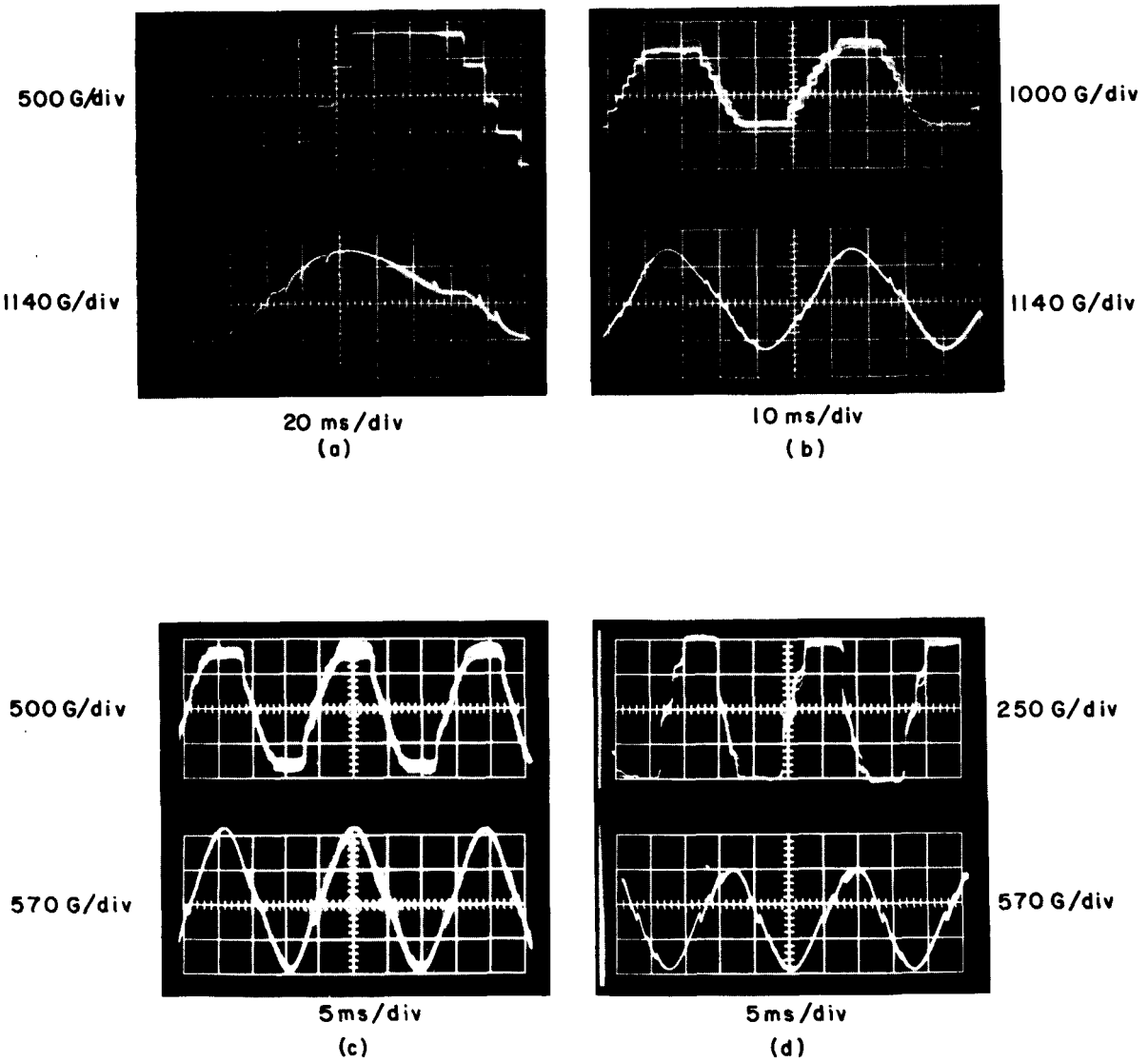

Figure III-12. ac Field Induced Flux Jumps when h is Large Enough to Cause More Than 2 Flux Jumps per Cycle

current of 10 microamps, was measured with a millimicrovoltmeter. The data are summarized in Table III-3.

The values of h shown in this table are equal to, or slightly less than, the values necessary to cause flux jumps at the respective frequencies. The changes in resistance of the carbon resistor which occur when such fields are applied for periods of up to several minutes are also shown. Recalling that the sensitivity of the resistor is about 40 Ω /degree, we see that the largest ΔR in this table corresponds to a temperature increase of 0.1 °K. It seems apparent from these data that there is no gross heating of the sample prior to the onset of flux jumping, even though the sample configuration in which temperature was measured probably constitutes a more severe thermal environment than that in which the flux jumping thresholds were measured. This is so because during the temperature measurements the liquid helium was not allowed to touch the interior surface. It seems safe to conclude on the basis of the data shown here that the ac field penetration effects described in section III-C of this report are occurring without a gross increase in temperature throughout the bulk of the sample. They, of course, do not preclude the possibility of a localized increase in temperature of sufficient magnitude to trigger the effects.

TABLE III-3. SAMPLE TEMPERATURE DURING APPLICATION OF ac FIELD

f (c/s)	h (gauss)	ΔR (Ω)	ΔT (°K)
20	650	-1	+.025
50	680	-2	+.05
200	430	-2	+.05
500	410	-4	+.10
1000	310	-3	+.075
2000	250	-2	+.05

Section IV

DISCUSSION OF RESULTS

A. RESULTS EXPECTED ON THE BASIS OF CRITICAL-STATE BEHAVIOR

In the process of interpreting the results obtained, it is useful to consider how a hard superconductor, in the mixed state, may behave in the presence of an ac field. Therefore, consider Figure IV-1(a) which shows a portion of the critical-state region of a typical tubular sample. Begin at point-zero (either by assuming that a flux jump has just occurred or by adjusting the dc field if necessary) and apply an ac field of amplitude somewhat less than h_1 so that the critical state is not reached. The ac field is shielded from the sample interior by the induced supercurrents. The field inside the sample remains constant although the external field is varying sinusoidally between $\pm h$. In a plot of H' (interior field) vs. H (external field), the point describing H' would move back and forth along the line $0\ 0'0''$ in Figure IV-1(a). No ac signal reaches the Hall probe under these circumstances. Now, however, if the amplitude of h is increased to a value greater than h_1, the sample will be placed in the critical state for a portion of each cycle. Flux will enter or leave the sample during those portions of the cycle when h is greater than h_1, and an ac signal will be detected by the Hall probe. The point representing H' will describe a loop such as ABDEG in Figure IV-1(a). The form of the signal reaching the detector in this example is important. This form is shown in Figure IV-1(c) for the applied signal in Figure IV-1(b). Note that: (1) no signal is recorded by the probe when h is less than h_1 (t_o to t_1 in Figure IV-1(c); (2) a signal, h', first reaches the probe when h becomes greater than h_1; (3) for the case where h is greater than h_1, h' follows h, that is, $\dot{h}' = \dot{h}$; (4) when h

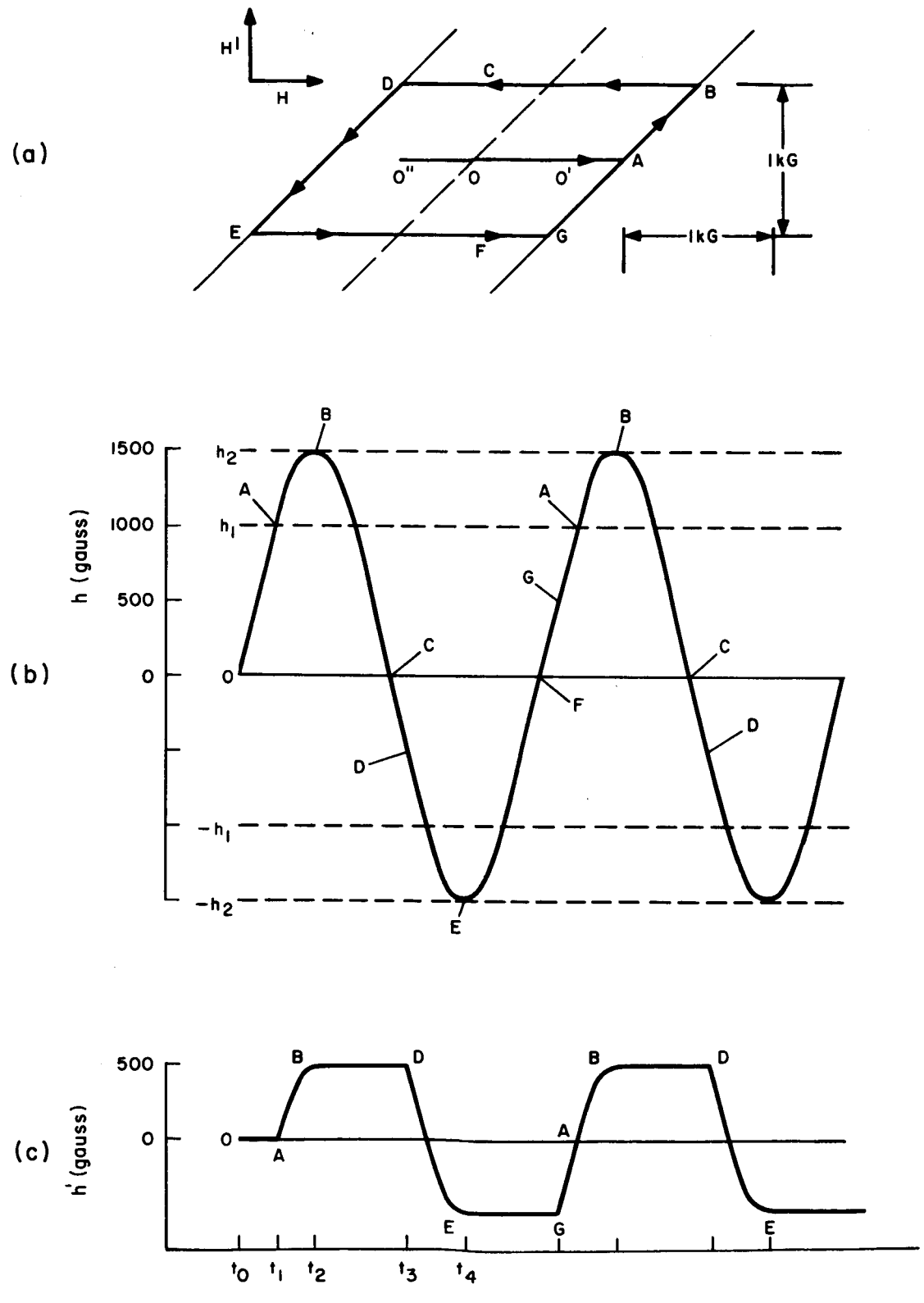

Figure IV-1. Penetration of an AC Field in the Manner Expected on the Basis of Critical State Performance.

begins to decrease, h' becomes constant (t_2 to t_3); and (5) when h becomes greater than h_1 in the negative-going portion of the cycle (t_3 to t_4) flux leaves the sample and h' again follows h. At no time during the cycle does $\dot{h}'$ exceed $\dot{h}$ and the amplitude of h' is equal to $h_2 - h_1$. Note also that the peak-to-peak amplitude of h must be greater than the width (in the H' vs. H plane) of the critical-state region before a signal will be detected by the Hall probe.

B. CONTRAST BETWEEN EXPECTED RESULTS AND ACTUAL OBSERVATIONS

The actual observations made at low frequencies (Figure III-9) are in agreement with these expectations in the following ways: (1) there exists a threshold value of h below which no ac component appears at the Hall probe; and (2) during each cycle (after ac has reached the sample interior) periods in which flux enters or leaves the sample alternate with those during which flux is shielded or trapped. The observations differ however in two most important respects: (1) the peak-to-peak variation in the ac signal required to cause a signal to appear at the Hall probe is significantly smaller than the width of the critical-state region; and (2) flux enters and leaves the sample in such a manner that $\dot{h}'$ is much greater than $\dot{h}$. For these reasons it is concluded that flux entrance and escape occur by means of flux jumping. Figure IV-2(a) shows a hysteresis loop in the H' vs. H plot which characterizes this ac field-induced flux jumping. This loop has been constructed from data contained in Figure III-9 (c). Part (b) of Figure IV-2 shows the ac signal which causes the flux jumps. The pips which occur during the momentary transistion to the normal state are shown also. The resultant square wave reaching the Hall probe is shown in part (c). From the reconstructed hysteresis loop in Figure IV-2, it can be seen that the flux jumps are imcomplete; i.e., not all of the shielded flux is admitted to the sample interior and not all the trapped flux is allowed to escape. Figure IV-3 shows, in an idealized manner, the hysteresis loop associated with an ac field of sufficient amplitude to produce more than two flux jumps per cycle.

The value of h' obtained from Figure III-9(c) is greater than 8×10^5 gauss/sec while the maximum time rate of change of the applied signal is $\dot{h} = 2.2 \times 10^5$ gauss/sec.

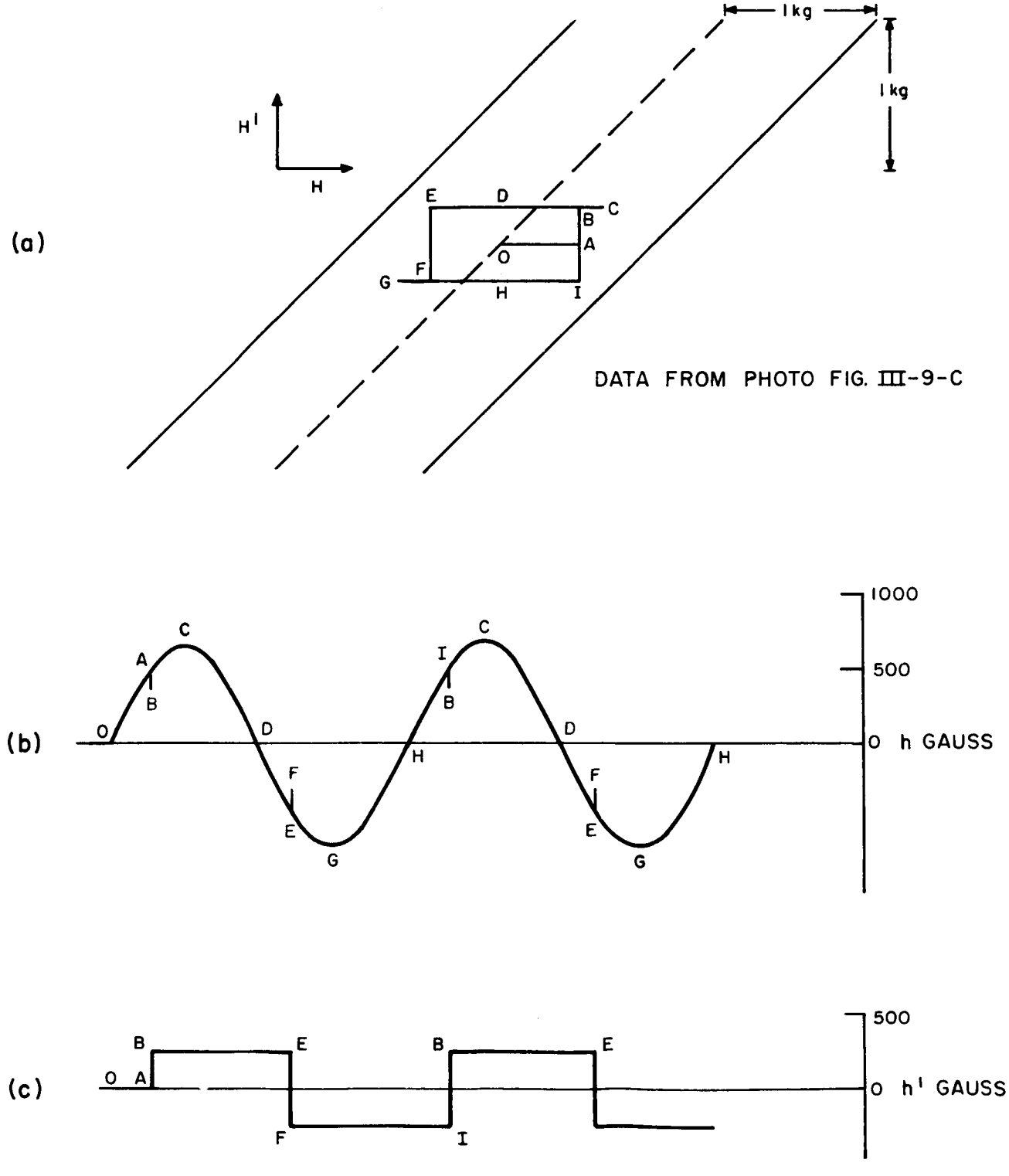

Figure IV-2. Observed AC Field Penetration Accompanied by Flux Jumps.

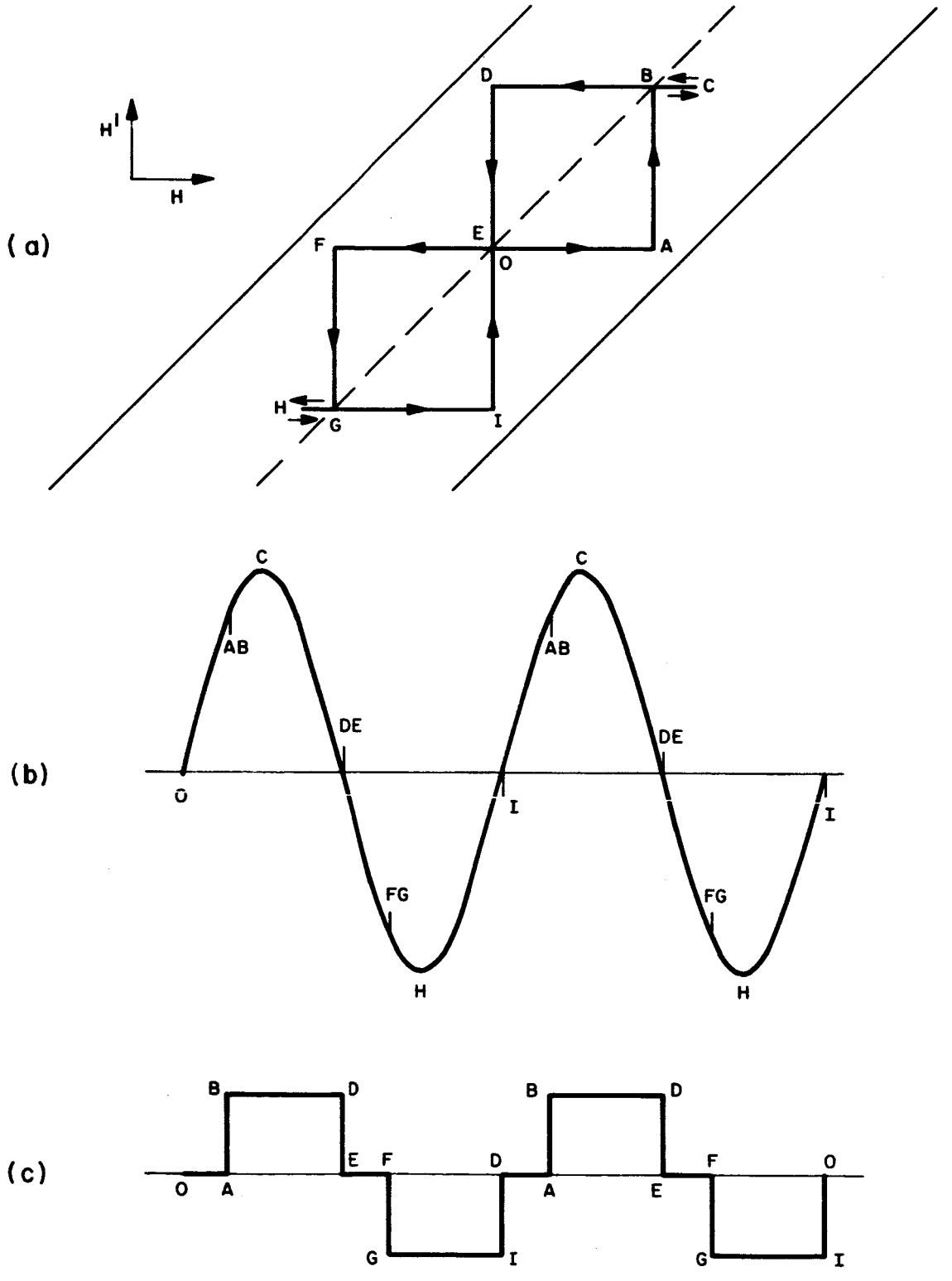

Figure IV-3. AC Field Penetration Accompanied by Two Flux Jumps Per Cycle (Idealized).

Data bearing on this point are summarized in Table IV-1. The data have been derived from the photos in Figure III-9. $\dot{h}$ has been evaluated at the point in the cycle when the pip appears in the waveform while $\dot{h}'$ is simply the magnitude of the flux jump divided by the estimated rise time of the square pulse.

TABLE IV - 1 RATES OF CHANGE OF APPLIED AND DETECTED FIELDS AT FLUX JUMPS

f (c/s)	$\dot{h}$ (gauss/sec)	$\dot{h}'$ (gauss/sec)
6.3	1.9×10^4	$>1.8\times10^5$
22	2.8×10^4	$>1.8\times10^5$
53	1.8×10^5	$>8.0\times10^5$
208	3.9×10^5	$\approx1.5\times10^6$

From figure III-9(d), for f=208 c/s, one may estimate the duration of a flux jump, using the rise time of the square wave on the Hall probe trace. The estimated duration is 2×10^{-4} sec. Using the estimated duration and the sample wall thickness one may define an effective velocity for the propagation of a flux jump which turns out to be 200 cm/sec.

Observations made at higher frequencies (f > several hundred c/s) again show that below a certain threshold field no alternating component appears at the Hall probe; the interior of the specimen is shielded from the ac field throughout the cycle. When the threshold is exceeded an ac component suddenly appears at the Hall probe. However in this case the signal at the Hall probe is a pure sine wave of amplitude nearly identical to that of h (see Figure III-10). Inasmuch as the form of the signal on the Hall probe exactly follows that of the applied signal, it is concluded that the specimen does not shield the ac field during any portion of its cycle. The amplitude of h 'is smaller than that of h by about 12 percent. It is believed that this is beyond the experimental error and may represent an energy loss to the specimen as the signal travels through it.

Viewing this behavior as an extension of that observed at the lower frequencies, one may assume that an extremely large number of very small flux jumps are occurring in rapid succession so that as far as can be observed h' and $\dot{h}'$ are following h and $\dot{h}$.

It is considered significant that the sine wave mode is observed when $\dot{h}_{max}$ becomes comparable to the value of $\dot{h}'$ during a flux jump. At f = 500 c/s where we observe the sine wave mode first, $\dot{h}_{max}$ is 1.3×10^6 gauss/sec, while our best estimate of $\dot{h}'$ during a flux jump is 1.5×10^6 gauss/sec.

C. FREQUENCY DEPENDENCE OF AC FIELD INDUCED FLUX JUMPS

In general, the value of h required to cause flux jumps at a particular frequency is inversely proportional to the frequency. This is true of both the square wave and sine wave modes. It also appears that this dependance is considerably stronger at the lower frequencies. The general features of the frequency dependance are illustrated in Figure IV-4 which is drawn for sample 5a from the data in Figures III-9, III-11, and III-13. The peak value of h at the onset of penetration in either mode is plotted against frequency and we note three distinct regions. For combinations of h and f in region I, the ac signal does not reach the interior of the specimen. For combinations of h and f in region II, two or more flux jumps per cycle occur in the square wave mode. In this region the specimen manifests extended periods of shielding behavior between flux jumps. For values of h and f in region III, the sine wave mode occurs and h' follows h throughout the cycle. There is no evidence of superconductive shielding behavior in this region. At the lower frequencies it is possible to observe all three regions as h is increased from zero. At higher frequencies a direct transition from region I to region III is made and it is not possible to observe region II. Apparently this mode, in which more or less identical flux jumps occur at regular intervals, is only stable at the lower frequencies. Regarding the form of the frequency dependence of h, it is noted that at low frequencies (below about 500 c/s) h goes inversely as a fractional power of f (along the curve defining the boundary between regions I and II, $h(f) \propto f^{-1/5}$) while at higher frequencies the dependence is almost linear.

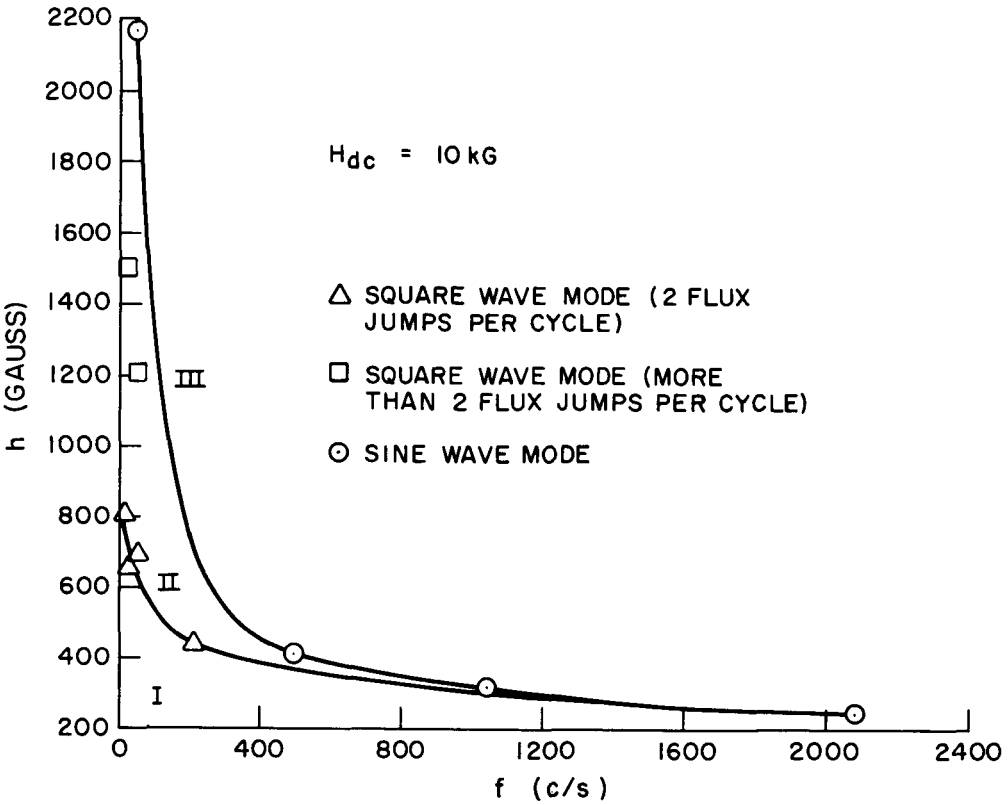

Figure IV-4. Frequency Dependence of the Threshold of Flux Jumping (Data for Sample 5a).

The photos in Figure III-9 show that the flux jump, as indicated by the pip in the applied signal waveform, occurs somewhat prior to the peak of the signal. Some relationship between h_p, the value of h at this point and $\dot{h}_p$ (which is ωh evaluated at the point where the pip occurs) is expected. The appropriate values are given in Table IV-2. We note that, with increasing frequency, h_p decreases while $\dot{h}_p$ increases. However, the decrease in h_p amounts to a factor of two while the increase in $\dot{h}_p$ is by more than a factor of ten. The nature of the relationship is not apparent from this.

TABLE IV-2. AMPLITUDE AND RATE OF CHANGE OF APPLIED FIELD AT FLUX JUMP

f (c/s)	h_p (gauss)	$\dot{h}_p$ (gauss/sec)
6.3	680	2×10^4
22	650	3×10^4
53	515	1.8×10^5
208	350	3.8×10^5

D. AMPLITUDE OF THE AC FIELD INDUCED FLUX JUMPS

We recall that flux jumps occur when a specimen is unstable to a small local increase in temperature. A perturbation will grow until a large portion of the sample is in the normal state thus permitting an avalanche of heretofore shielded flux to enter the interior of the sample or of trapped flux to leave. Since the parameter α, which is a measure of the strength of pinning, is inversely proportional to temperature, a slight increase in temperature results in a local reduction in pinning center strength and allows a quantity of pinned flux to move past the pinning center. This flux motion is dissipative so that more heat is added locally, resulting in a further increase in temperature and consequent release of more flux. If the thermal conductivity of the material is such that the locally generated heat is not removed from the hot spot quickly enough, the local temperature will increase, the hot spot will grow, and the process continues until a large part of the sample is driven into the normal state with the release of all pinned flux from the normal region. Once all the pinned flux has been released, the internal heat source of the specimen no longer exists; if the sample is in good thermal contact with an ambient temperature less than T_c, it will return immediately to the superconducting state. In the light of the expected random character of the flux jumps, the reproducibility manifested by our data is quite remarkable. Flux jumps occur under the same conditions during each cycle, and the field change in the interior of the specimen is the same in cycle after cycle.

From this point of view it is interesting to note the relative constancy of the amplitude of the flux jumps even though the amplitude and frequency of h necessary to produce them vary over a considerable range. Table IV-3 is a summary of data from Figure III-9 relevant to this point. Also relevant are the data in Figure III-12 which are summarized in Table IV-4. Although one flux jump of 200 gauss and two flux jumps of 350 gauss occur it is noted that a strong concentration of data points is evident in the region from 400 to 500 gauss. This magnitude would appear to be characteristic of the specimen.

TABLE IV-3. AMPLITUDE OF FLUX JUMPS (DATA FROM FIGURE III-9)

f (c/s)	h (gauss)	$\Delta h'$ (gauss)
6.3	800	450
22	655	450
53	685	500
208	430	370

TABLE IV-4. AMPLITUDE OF FLUX JUMPS (DATA FROM FIGURE III-12)

f (c/s)	h (gauss)	$\Delta h'$ (gauss)
6	1570	450 450 500 400
22	1395	500 500 475
53	1540	450 500 350 200 350 400

E. PRACTICAL CRITICAL CURRENT DENSITY IN THE PRESENCE OF SUPERIMPOSED AC AND DC FIELDS

In previous work a practical critical-current density in dc fields has been defined as that current which exists immediately prior to a flux jump. In an analogous manner a practical critical-current density in the ac field may be defined as being that which is flowing when the threshold for ac field-induced flux jumping is reached. With the data in Figure III-9 for example, one can compute this from:

$$(J_c)_{ac} = \frac{h}{0.4\ \pi\ w}$$

where h is the peak amplitude of the ac field immediately before the onset of flux jumping. The practical critical-current data for f = 53 c/s are summarized in Table IV-5 which also lists, for comparison, the critical-current density in a dc field. It is considered noteworthy that the three values of $(J_c)_{ac}$ thus computed are a reasonably good fit to an equation of the form of Kim's semi-empirical expression for the critical-current density:

$$J_c = \frac{\alpha_c}{H + B_o}$$

This is demonstrated in Figure IV-5 in which we have plotted $1/J_c$ against H and obtained a reasonably good straight line. The slope of this line is equal to $(\alpha_c)^{-1}$ and the y-axis intercept is equal to B_o/α_c. This fit may indicate that the flux jumps occur just as the specimen is about to enter a critical state which has been modified by the ac field.

It can be seen from the data in Table IV-5 that α_c for f = 53 c/s is somewhat smaller than α_c for dc while B_o for the ac field data is slightly greater than that for the dc case.

Similar computations have been carried out for sample 5 (based on the early data described in Section III-c of this report) and they are summarized in Table IV-6. While the values of α_c and especially of B_o derived from the ac data seem unusually large in this case, it is still significant that the $1/J_c$ vs. H plots, shown in Figure IV-6, are reasonably close to straight lines.

TABLE IV-5. PRACTICAL CRITICAL STATE DATA FOR f = 53 c/s (SAMPLE 5a)

H (kG)	(J_c)ac (A/cm^2)	(J_c)dc (A/cm^2)	α_c (kG-A/cm^2)		B_o (kG)	
			53 c/s	dc	53 c/s	dc
5	1.6×10^4	2.9×10^4				
10	1.2×10^4	2.1×10^4	$.30 \times 10^6$	$.46 \times 10^6$	14.4	11.0
20	0.90×10^4	1.5×10^4				

F. AC POWER LOSSES IN THE TEST SAMPLES

1. Hysteresis Losses

Figure IV-7(b) shows the field distribution in the wall of a sample during a cycle of the alternating field (Figure IV-7(a)). (It has been assumed that there is no field gradient within the wall of the sample to begin with; this assumption does not

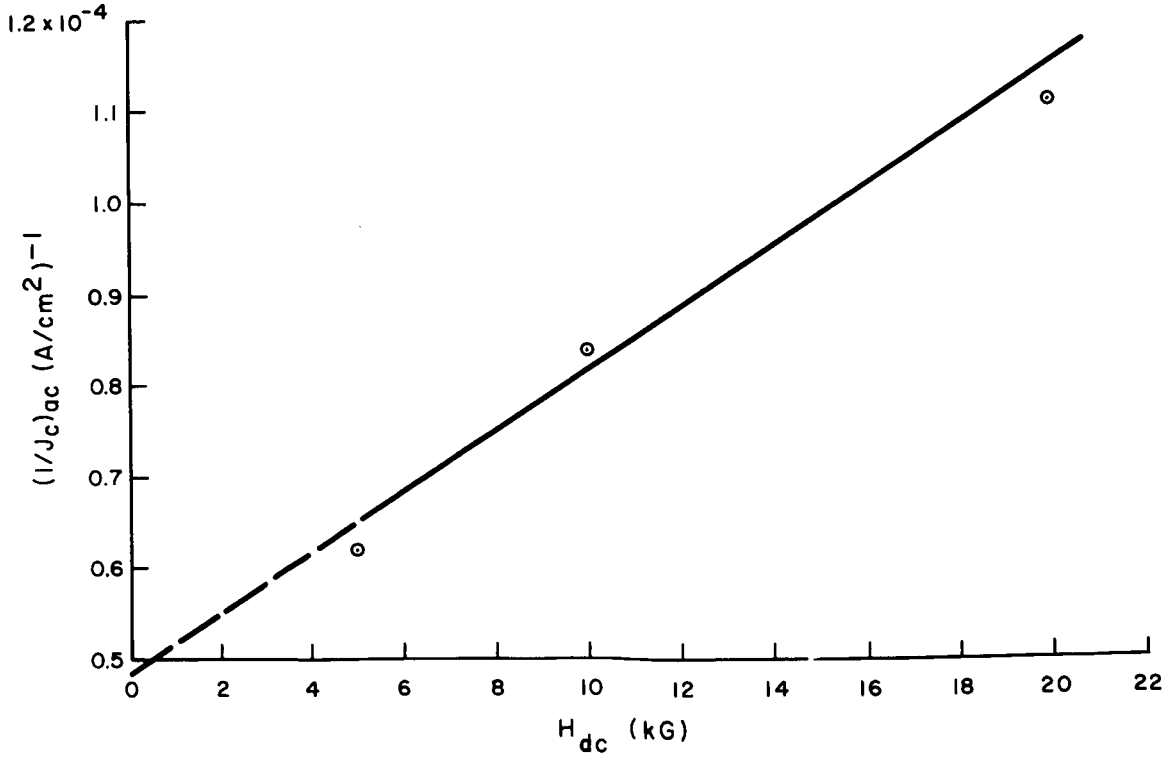

Figure IV-5. Showing the Proximity of Experimental Points to a Line Representing Kim's Equation (sample 5a)

TABLE IV-6. PRACTICAL CRITICAL STATE DATA (SAMPLE 5)

H	$(J_c)_{ac}$ (A/cm^2)			σ_c (kG-A/cm^2)			B_o (kG)		
(kG)	20 c/s	50 c/s	100 c/s	20 c/s	50 c/s	100 c/s	20 c/s	50 c/s	100 c/s
				$.85 \times 10^6$	$.56 \times 10^6$	$.45 \times 10^6$	60.5	45.4	40.9
5	1.4×10^4	1.1×10^4	0.98×10^4						
10	1.1×10^4	1.0×10^4	0.87×10^4						
15	1.1×10^4	0.9×10^4	0.79×10^4						
20	1.1×10^4	0.85×10^4	0.74×10^4						
25	1.0×10^4	0.79×10^4	0.69×10^4						

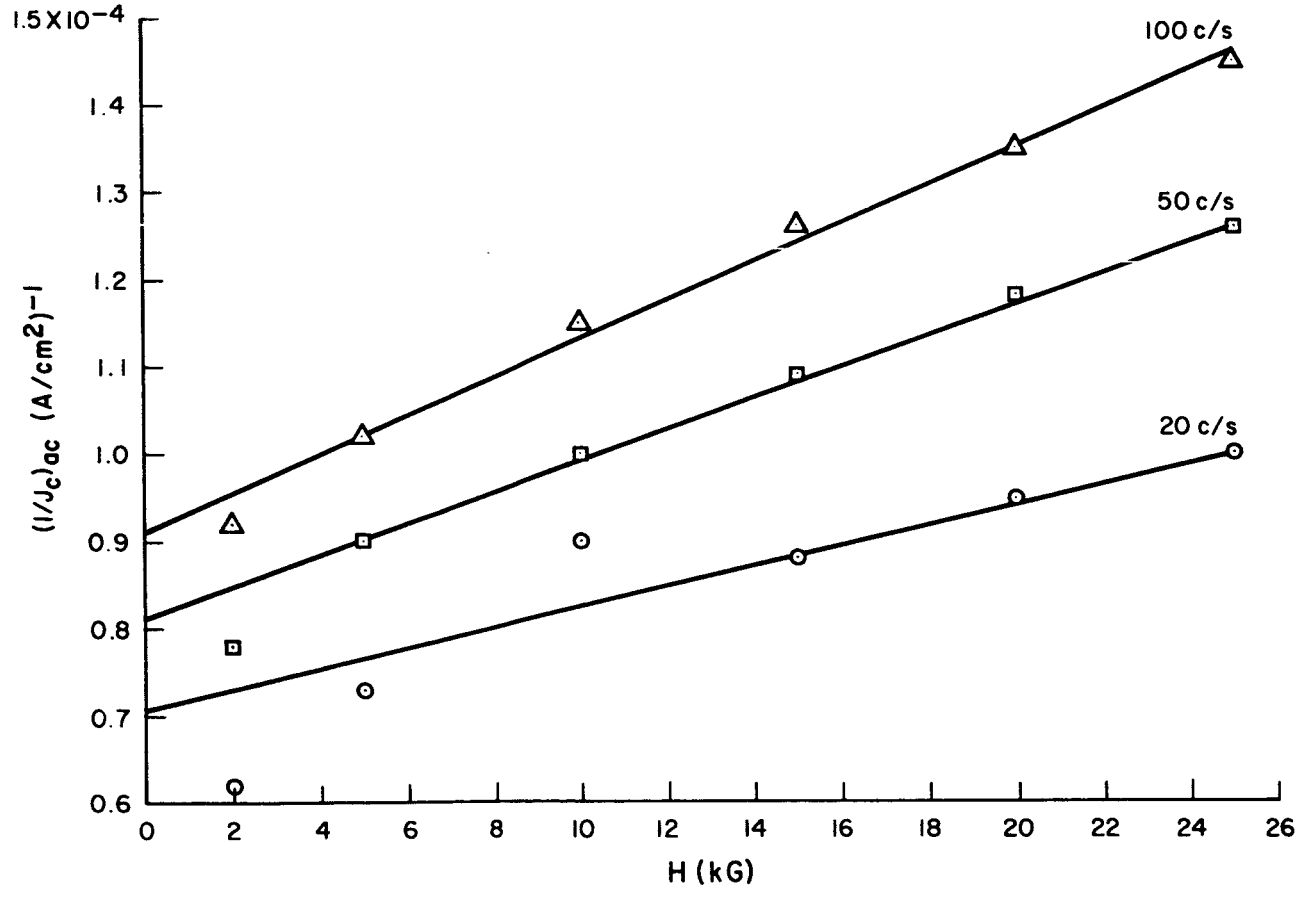

Figure IV-6. Showing the Proximity of Experimental Points to Lines Representing Kim's Equation (sample 5)

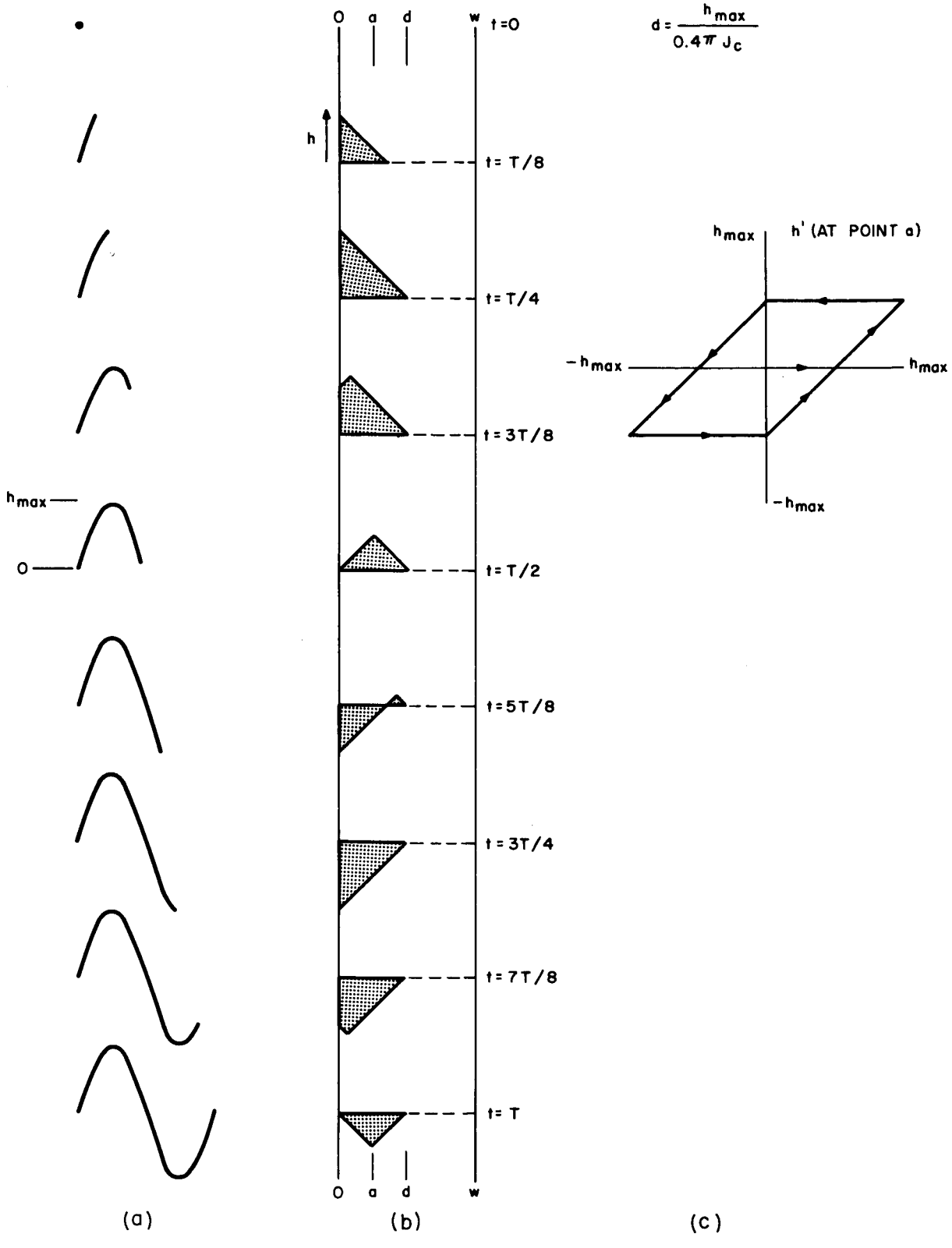

Figure IV-7. Field Changes in Specimen Wall During Cycle of ac Signal, Illustrating Hysteresis Associated with Field Dependent Penetration Depth

affect the result.) In this example the amplitude of h and the critical-current density are such that the field penetrates to a depth equal to half the thickness of the specimen. The field at depth, a, is shown in Figure IV-7(c). We note the hysteresis associated with the field dependent penetration depth. During each cycle the specimen absorbs an amount of energy proportional to the integral, $\oint$ HdB. After Bean, [5] the energy loss per unit volume per cycle is given by

$$W = \frac{H_o^3}{3\pi H^*} - \frac{5 H_o^4}{16\pi H^{*2}} \text{ ergs/cm}^3\text{/cycle}$$

where

H_o = maximum amplitude of ac field in gauss

H^* = $0.4\pi J_c w$ = field necessary to cause penetration to interior surface.

The total power per unit volume dissipated in the specimen is $P = Wf$, where f is the frequency. Computations of the power being dissipated just prior to the onset of flux jumps are summarized in Table IV-7. These computations refer to both the square wave mode and the sine wave mode. It is interesting to note that the energy per cycle is constant within a factor of about 3 over the frequency range from 6 to 208 c/s. However the power, which is proportional to the frequency, is more than a factor of 10 greater at 208 c/s than at 6.3 c/s. The amplitude of the signal at 208 c/s is about half that at 6.3 c/s so the penetration depth is about half. If hysteresis losses were the mechanism by which flux jumps were triggered one might conclude from this that it is easier to trigger a jump deep within the material than near the surface.

At the higher frequencies (500-to-2080 c/s), the situation differs in that the energy per cycle decreases but the total power is very nearly constant.

TABLE IV-7. HYSTERESIS LOSSES AT THE THRESHOLD OF FLUX JUMPING (SAMPLE 5)

	f (cps)	h (gauss)	W $\frac{\text{joules}}{\text{cm}^3 - \text{cycle}}$	P $\frac{\text{watts}}{\text{cm}^3}$
square wave mode	6.3	800	13.8×10^{-4}	8.7×10^{-3}
	22	655	11.5×10^{-4}	2.5×10^{-2}
	53	685	12.2×10^{-4}	6.5×10^{-2}
	208	430	5.0×10^{-4}	1.0×10^{-1}
sine wave mode	500	410	4.5×10^{-4}	2.3×10^{-1}
	1040	308	2.2×10^{-4}	2.3×10^{-1}
	2080	245	1.2×10^{-4}	2.5×10^{-1}

2. Eddy Current Losses

We now consider, as a mechanism for the triggering of flux jumps, eddy current losses associated with the changing magnetic field in the sample. The field is changing within a depth, d, given by:

$$d = \frac{h}{0.4 \pi J_c}$$

where h is the amplitude of the ac field at the threshold and J_c is the critical-current density obtained from the dc critical-state curves. Within this depth the changing field gives rise to an induced electric field.

The induced field is

$$E = \frac{-\dot{B} A}{2 \pi r}$$

where A = the area of the annular region in which the field is changing.

r = the average radius of the annular region.

$\dot{B} = \omega$ Bo cos ω t

The rms power density associated with this field is

$$P_{rms} = \frac{E_{rms}^2}{\rho}$$

$$= (5 \times 10^{-13}) \frac{\omega^2 B_o^2 A^2}{(2\pi r)^2 \rho} \text{ watt/cm}^3$$

P_{rms} is given in watt/cm^3 if B_o = h gauss, A is in meters^2, r is in meters and ρ is in ohm-centimeters.

We have computed P_{rms} using $\rho = 8.6 \times 10^{-5}$ Ω cm, a value obtained by Berlincourt and Hake[6] for NbTi; in the normal state at 1.2°K. The computations are summarized in Table IV-8.

We note that the normal eddy current losses are very much smaller than the computed hysteresis losses in Table IV-7. Use of a flux flow resistivity,[8] $\rho_f = \rho \frac{H}{H_{c2}}$, results in an increase in eddy current losses of about a factor of ten since ρ_f is about 0.1 ρ_n for H = 10 kG. A smaller flux flow resistance, found where ρ is in transition from a value of zero to the value, $\rho \frac{H}{H_{c2}}$, would lead to a correspondingly larger eddy current loss.

TABLE IV-8. EDDY CURRENT LOSSES

	f (c/s)	P_{rms} (watts/cm^3)
Square Wave Mode	6.3	5.34×10^{-7}
	22	2.90×10^{-6}
	53	2.02×10^{-5}
	208	4.95×10^{-5}
Sine Wave Mode	500	2.34×10^{-4}
	1040	3.32×10^{-4}
	2080	5.38×10^{-4}

3. Sample Temperature Rise

In order to estimate the temperature rise associated with power dissipation in the specimen, we consider the heat conduction equation under the following simplifying conditions (see Figure IV-8): (1) we treat the problem one dimensionally, (2) we assume that the power dissipated in region I (where the field penetrates) is distributed uniformly throughout this region, and (3) we consider the steady state case, $\partial T/\partial t = 0$.

The solutions are summarized in Figure IV-9 which shows the normalized temperature distribution in the wall of the specimen.

The parameter A may be evaluated from

$$A = - \frac{P d^2}{2 \varkappa}$$

where

P = power dissipated per unit volume (in watts/cm^3)

$\varkappa$ = thermal conductivity and is estimated to be 10^{-2} watts/cm - degree K.

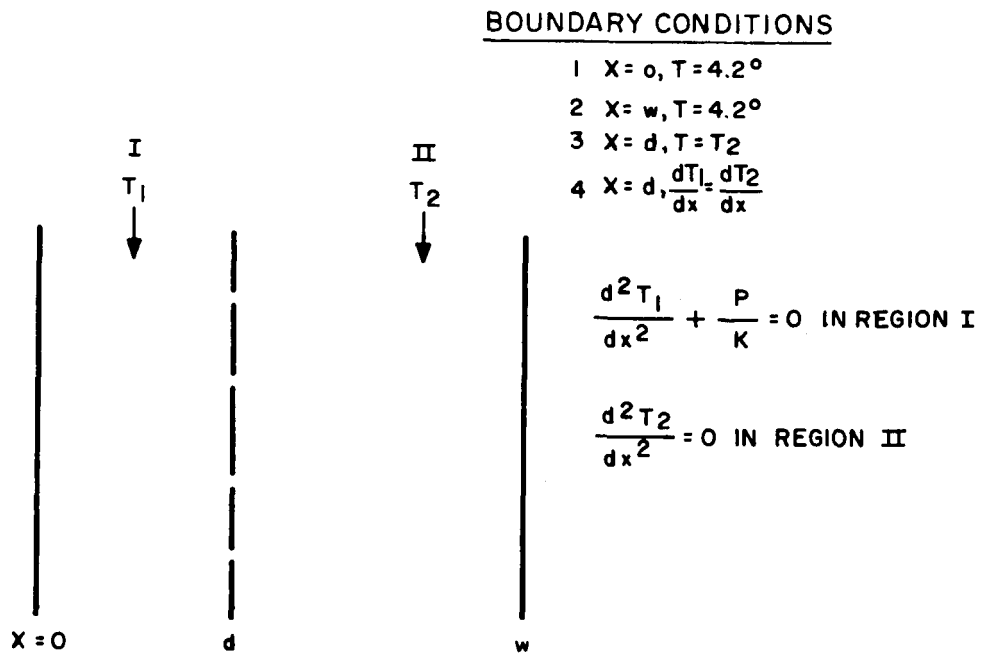

Figure IV-8. Simplified Approach to Computation of Temperature Increase in Specimen

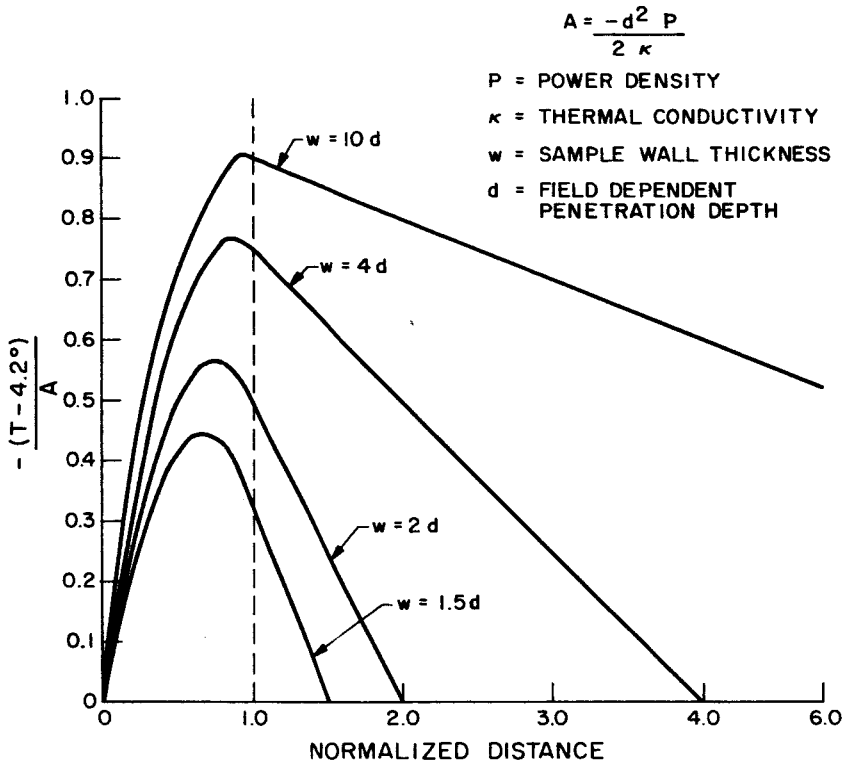

Figure IV-9. Normalized Temperature Increase in Specimen as a Function of Normalized Position in Specimen Wall

Using this figure we may compute the temperature increases associated with hysteresis and eddy current losses. For f = 2080 c/s, h = 245 G so that the curve labelled w = 4d is appropriate. The power dissipated in hysteresis losses is 2.3×10^{-1} watts/cm^3. This leads to a maximum temperature increase of 0.76 millidegree. It appears that hysteresis losses can not cause a large enough temperature increase to account for our observations even if allowance is made for the rough assumptions and approximations made in the computations.

For eddy current losses associated with the normal resistivity, the temperature increase would be even smaller. However the use of a flux flow resistance combined with a more accurate computation (in which conditions (2) and (3) were relaxed) might lead to a significantly large temperature increase. This seems rather speculative at present. Perhaps all one may conclude from these computations is that the initiation of a flux jump is such a highly localized phenomenon that a consideration of the average macroscopic temperature increase does not give a sufficiently accurate picture.

Section V

CONCLUSIONS AND RECOMMENDATIONS

A. SUMMARY OF FINDINGS

Magnetization experiments in superimposed ac and dc fields have yielded much interesting information about the manner in which a hard superconductor shields an alternating field. Before the ac experiments were performed, it was determined through dc magnetization experiments that the NbTi tubes were "well-behaved" hard superconductors. They exhibited a field-dependent, critical-current density that was consistent with Kim's semi-empirical expression $J_c = \alpha_c/(H + B_o)$ and values of α_c and B_o for the different samples were in reasonably good agreement. When exposed to an ac field, a sample shielded its interior as long as the ac field amplitude, h, remained below a certain threshold. When this threshold (which was smaller than the dc field which could be shielded) was exceeded, flux rushed into (and out of) the sample in a precipitous manner identified as flux jumping. At low frequencies (f < several hundred c/s) no flux entered or left the specimen interior during any portion of the cycle other than the instant at which the flux jumps occurred. Square waves caused by two flux jumps per cycle were observed, by means of a Hall probe within the sample, and displayed on an oscilloscope. At higher frequencies (f > several hundred c/s) flux entered and left the specimen throughout the cycle and a sine wave, similar in amplitude to the applied signal, was detected by the Hall probe. At low frequencies it was possible to observe a multitude of well defined flux jumps per cycle by increasing the amplitude of h. At low frequencies the duration of the flux jumps was estimated at 2×10^{-4} sec and this was believed to be a fairly general property of the specimen. The flux jumps were strikingly similar in amplitude over a range of frequencies (6.3 to 208 c/s) and amplitudes

(430 to 2200 gauss) of the ac field; the most frequently observed values were in the interval from 400 to 500 gauss. h (f) at the onset of flux jumping varied inversely with frequency from 6.3 to 2080 c/s with the dependence being stronger, at lower frequencies. h (H_{dc}) at the onset of flux jumping varied inversely with the dc field ($2,000 < H < 25,000$ G) with the dependence being stronger at lower fields. The practical critical-current density in the superimposed ac and dc fields is smaller than the true value in the dc field alone by a factor between 1.2 (low frequency) and about 4 (high frequency). Several mechanisms by which the ac field might dissipate power in the specimens have been considered and the computed hysteresis losses associated with the field dependent penetration depth are far greater than the normal eddy current losses. Temperature increases associated with ac power losses have been computed (for a much simplified situation), and these average temperature increases are not great enough to bring the temperature of any part of the sample up to T_c. This result is in qualitative agreement with temperature measurements made with a carbon resistor which indicates that no significant temperature rise at the inner surface occurs prior to penetration of the ac field to the interior of the sample. This does not rule out the possibility of a highly localized temperature increase which might be revealed by a more realistic calculation.

B. RECOMMENDATIONS FOR FURTHER INVESTIGATION

The results of the experiments described above have indicated a number of areas in which further effort might profitably be expended. It is believed that similar experiments should be performed for samples with very much different wall thickness than have thus far been studied. It is possible that if the sample wall is made thin enough, flux jumps may not occur at all for a certain range of frequencies; therefore, one may measure the true ac critical current density (not a practical critical current such as we have talked about) directly, as a function of frequency, dc field, and temperature. In this vein it should also be of interest to observe the penetration of sinusoidally varying fields at frequencies from 6.3 c/s (the lower limit of the present investigation) down to a fraction of a cycle per second.

Samples with surface characteristics which have been modified by plating, polishing, and etching should be studied to obtain information on the role the surface plays in the triggering of flux jumps. Having determined the role of the surfaces, one should investigate the importance of bulk structure changes such as might accompany heat treatment of heavily worked material. To shed more light on the expected relationship between the field gradient in the sample (as determined by the amplitude of the ac field) and the rate of change of field at the instant when a flux jump occurs, one should observe the penetration of non-sinusoidally varying fields such as ramps and square waves. If it is possible to find a regime in which pulses are transmitted without causing flux jumps, one may observe the transmission time of such pulses and attempt to relate this time to the flux flow velocity and resistance.

The present investigation has enabled us to estimate the duration of a flux jump. It would be of great interest to study this duration under a variety of thermal conditions such as higher temperatures and lack of direct contact between the specimen and the helium bath. Also, it may be possible to observe a resistive transition during the flux jump.

ACKNOWLEDGEMENTS

The authors wish to acknowledge the contributions of Dr. G. D. Cody of RCA Laboratories and Professor C. A. Domenicali and Dr. L. Dubeck of Temple University who provided useful suggestions and discussions. Dr. R. Hecht, now of National Research Corp., suggested the use of the tickler coil as an experimental technique.

REFERENCES

1. C. M. Harper and R. Hecht, "Study of Properties of High-Field Superconductors at Elevated Temperatures", Technical Summary Report on NASA Contract NAS 8-11272, 26 July, 1965.

2. Y. B. Kim, C. F. Hempstead, and A. R. Strnad, "Flux Creep in Hard Superconductors", Phys. Rev. 131, 2486 (1963).

3. Private Communication, D. Fox, Westinghouse Research Labs., Dec. 1965.

4. F. E. Hoare, L. C. Jackson and N. Kurti, "Experimental Cryophysics", Butterworths & Co., London, 1961.

5. C. P. Bean, "Magnetization of High Field Superconductors", Reviews of Modern Physics 36, 31 (1964).

6. T. G. Berlincourt and R. R. Hake, "Superconductivity at High Magnetic Fields", Phys. Rev. 131, 140 (1963).

7. P. W. Anderson, "Theory of Flux Creep in Hard Superconductors", Phys. Rev. Letters 8, 250 (1962).

8. Y. B. Kim, C. F. Hempstead, and A. R. Strnad, "Flux Flow Resistance in Type-II Superconductors", Phys. Rev. 139, A1163 (1965).